

Dystroglycan Maintains Inner Limiting Membrane Integrity to Coordinate Retinal Development

Reena Clements¹, Rolf Turk³, Kevin P. Campbell³, and Kevin M. Wright^{1,2, #}

1) Neuroscience Graduate Program, 2) Vollum Institute, Oregon Health & Science University, Portland, OR 97239, USA, 3) Howard Hughes Medical Institute, Department of Molecular Physiology and Biophysics, Department of Neurology, Department of Internal Medicine, The University of Iowa Roy J. and Lucille A. Carver College of Medicine, Iowa City, IA USA.

#) Correspondence to Kevin M Wright (wrightke@ohsu.edu). Vollum Institute, 3181 SW Sam Jackson Park Rd L474 Portland, OR 97239. (503)-494-6955

Running Title:

Dystroglycan regulates retinal development

Abstract

Proper neural circuit formation requires the precise regulation of neuronal migration, axon guidance and dendritic arborization. Mutations affecting the function of the transmembrane glycoprotein dystroglycan cause a form of congenital muscular dystrophy that is frequently associated with neurodevelopmental abnormalities. Despite its importance in brain development, the precise role for dystroglycan in regulating retinal development remains poorly understood. Using a mouse model of dystroglycanopathy (*ISPD^{L79*}*) and conditional *dystroglycan* mutants, we show that dystroglycan is critical for the proper migration, axon guidance and dendritic stratification of neurons in the inner retina. Using genetic approaches, we show that dystroglycan functions in neuroepithelial cells as an extracellular scaffold to maintain the integrity of the retinal inner limiting membrane (ILM). Surprisingly, despite the profound disruptions in inner retinal circuit formation, spontaneous retinal activity is preserved. These results highlight the importance of dystroglycan in coordinating multiple aspects of retinal development.

1 **Introduction**

2 The precise lamination of neurons is a common organizing principle of the
3 vertebrate nervous system and is critical for establishing proper connectivity. In many
4 regions of the developing nervous system, newly generated neurons migrate in a basal
5 direction away from apically located proliferative zones. In the developing retina,
6 progenitor cells localized in the apical neuroepithelium undergo asymmetric cell
7 divisions to produce a variety of retinal cell types in a sequential manner (Reese, 2011).
8 Retinal ganglion cells (RGCs), the sole output cells of the retina, are generated first in
9 early embryonic development, followed by horizontal cells and cones. Rods, amacrine
10 cells, bipolar cells and Müller glia are the last to differentiate (Bassett and Wallace,
11 2012; Livesey and Cepko, 2001; Reese, 2011). In contrast to the developing cortex,
12 birthdate order does not predict the laminar placement of neurons within the retina.
13 Rather, the retina is organized in three major cellular layers: the apically located outer
14 nuclear layer (ONL) comprised of rod and cone photoreceptors; the inner nuclear layer
15 (INL) containing horizontal cells, bipolar cells and amacrine cells; and the basally
16 located ganglion cell layer containing RGCs and displaced amacrine cells (Bassett and
17 Wallace, 2012). Two synaptic lamina form postnatally in the retina: the outer plexiform
18 layer (OPL), which contains synapses between photoreceptors, bipolar cells and
19 horizontal cells; and the inner plexiform layer (IPL), which contains synapses between
20 bipolar cells, amacrine cells and RGCs. The molecular cues that direct the stratification
21 of neuronal subtypes and their processes in the retina remain poorly understood.

22 Unlike the cerebral cortex, where many neurons migrate along the radial glia
23 scaffold, neuronal migration in the retina does not require contact between neurons and

24 neuroepithelial cells (Reese, 2011). RGCs, bipolar cells and photoreceptors migrate by
25 nuclear translocation through a basally-directed process, while amacrine cells and
26 horizontal cells migrate without obvious processes directed towards either the apical or
27 basal surface of the retina. Basal process contact with the inner limiting membrane
28 (ILM) is critical for the polarization and migration of RGCs (Randlett et al., 2011). RGC
29 axons form in the optic fiber layer (OFL), along the laminin-enriched ILM, and direct
30 their axon growth to the optic disc at the center of the retina (Bao, 2008). The ILM is
31 made up of various extracellular matrix (ECM) proteins including laminins, Collagen IV,
32 nidogens, perlecan, and agrin (Taylor et al., 2015; Varshney et al., 2015). Mutations in
33 specific laminins (Lam α 1, Lam β 2 and Lam γ 3) or the laminin receptor β 1-Integrin, disrupt
34 formation of the ILM and organization of the ganglion cell layer (GCL) (Edwards et al.,
35 2010; Gnanaguru et al., 2013; Pinzon-Duarte et al., 2010; Riccomagno et al., 2014).
36 How laminins and other ECM proteins are initially organized in the ILM remains unclear.

37 In addition to β 1-Integrin, the transmembrane glycoprotein dystroglycan functions as
38 a receptor for laminins and other ECM proteins that contain Laminin G (LG) domains
39 through its extracellular α -subunit. Dystroglycan also connects to the actin cytoskeleton
40 through the intracellular domain of its transmembrane β -subunit, which is part of the
41 dystrophin glycoprotein complex (Moore and Winder, 2010). The extensive
42 glycosylation of dystroglycan's α -subunit is essential for its function, with the mature
43 glycan chains binding to LG motifs present in a number of ECM proteins (Moore and
44 Winder, 2012). Mutations in one of 17 genes encoding proteins required for the
45 functional glycosylation of dystroglycan lead to a form of congenital muscular dystrophy
46 termed dystroglycanopathy (Taniguchi-Ikeda et al., 2016). Patients with

47 dystroglycanopathy can present a wide range of symptoms, and the most severe forms,
48 Muscle-Eye-Brain disease (MEB) and Walker Warburg Syndrome (WWS), are
49 accompanied by significant neurological involvement (Godfrey et al., 2011). MEB and
50 WWS are characterized by cortical malformation (type II lissencephaly), cerebellar
51 abnormalities, and retinal dysplasias (Dobyns et al., 1989).

52 Cortical malformations in dystroglycanopathies have been well-studied, and reflect
53 neuronal migration defects that arise from the critical role that dystroglycan plays in
54 maintaining the architecture of the neuroepithelial scaffold (Moore et al., 2002; Myshra
55 et al., 2012). In several mouse models of dystroglycanopathy, focal regions of retinal
56 dysplasia have been observed, with ectopic cells protruding through the ILM (Chan et
57 al., 2010; Lee et al., 2005; Satz et al., 2008; Takahashi et al., 2011; Takeda et al.,
58 2003). However, several important questions regarding the role of dystroglycan in
59 retinal development remain unaddressed. First, is dystroglycan required for the proper
60 migration and lamination of specific subtypes of retinal neurons? Second, is
61 dystroglycan required to maintain the ILM as a growth substrate for RGC axons as they
62 exit the retina? Third, how does the loss of dystroglycan affect the postnatal dendritic
63 stratification and mosaic spacing of retinal neurons? Finally, how do the retinal
64 dysplasias present in models of dystroglycanopathy affect the function of the retina?

65 Here, using multiple genetic models, we identify a critical role for dystroglycan in
66 multiple aspects of retinal development. We show that dystroglycan within the
67 neuroepithelium is critical for maintaining the structural integrity of the ILM. We provide
68 *in vivo* evidence that dystroglycan's maintenance of the ILM is required for proper
69 neuronal migration, axon guidance and the postnatal formation of synaptic lamina

70 specifically within the inner retina. Surprisingly, spontaneous retinal activity appears
71 unperturbed, despite the dramatic disruption in inner retinal development. Together,
72 these results provide critical insight into how dystroglycan directs the proper functional
73 assembly of retinal circuits.

74

75 **Results**

76

77 **Dystroglycan is required for inner limiting membrane integrity and axon tract** 78 **formation in the developing retina**

79 Dystroglycan plays a critical role in the developing cortex, where it anchors radial
80 neuroepithelial endfeet to the basement membrane along the pial surface. In the
81 absence of functional dystroglycan, disruptions in the cortical basement membrane and
82 detachment of neuroepithelial endfeet lead to profound neuronal migration phenotypes
83 (Moore et al., 2002; Myshra et al., 2012). In the adult retina, dystroglycan is present in
84 blood vessels, in RGCs, at ribbon synapses in the OPL, and at the ILM, which serves as
85 a basement membrane that separates the neural retina from the vitreous space
86 (Montanaro et al., 1995; Omori et al., 2012). However, the role of dystroglycan in
87 regulating neuronal migration, axon guidance or dendritic stratification of specific cell
88 types during retinal development has not been examined in a comprehensive manner.
89 To address this open question, we first examined the expression pattern of dystroglycan
90 in the developing retina. Using immunohistochemistry, we observed dystroglycan
91 expression along radial processes that span the width of the retina, and its selective
92 enrichment at the ILM from embryonic ages (e13) through birth (P0) (Figure 1A). These
93 processes are likely a combination of neuroepithelial cells and the basal process of
94 migrating RGCs. Loss of staining in retinas from an epiblast-specific *dystroglycan*

95 conditional knockout ($DG^{F/-}; Sox2^{cre}$) confirmed the specificity of this expression pattern
96 (Figure 1A).

97 The first step in the assembly of basement membranes is the recruitment of laminin
98 polymers to the cell surface by sulfated glycolipids, followed by the stabilization of
99 laminin polymers by transmembrane receptors (Yurchenco, 2011). To determine
100 whether dystroglycan is required for the initial formation of the ILM during retinal
101 development, we utilized two complementary genetic models. $ISPD^{L79*/L79*}$ mutants,
102 previously identified in a forward genetic screen, lack the mature glycan chains required
103 for dystroglycan to bind ligands such as laminin and are a model for severe
104 dystroglycanopathy (Wright et al., 2012). $DG^{F/-}; Sox2^{cre}$ conditional mutants lack
105 dystroglycan in all epiblast-derived tissues and were utilized to confirm that phenotypes
106 observed in $ISPD^{L79*/L79*}$ mice are dystroglycan dependent. The enrichment of laminin at
107 the ILM appeared normal in early retinal development at e13 in both $ISPD^{L79*/L79*}$ and
108 $DG^{F/-}; Sox2^{cre}$ mutants (Figure 1B-D), indicating that dystroglycan is not required for the
109 initial formation of the ILM. However, at e16, we observed a profound loss of laminin
110 staining and degeneration of the ILM across the entire surface of the retina in
111 $ISPD^{L79*/L79*}$ and $DG^{F/-}; Sox2^{cre}$ mutants (Figure 1C-D, Supplemental Figure 1). The
112 loss of ILM integrity in $ISPD^{L79*/L79*}$ and $DG^{F/-}; Sox2^{cre}$ mutants was accompanied by the
113 inappropriate migration of retinal neurons, resulting in the formation of an ectopic layer
114 of neurons protruding into the vitreous space.

115 Following the initial polymerization of laminin on cell surfaces, additional ECM
116 proteins bind and crosslink the nascent basement membrane to increase its stability
117 and complexity. Examination of $ISPD^{L79*/L79*}$ mutant retinas at P0 revealed a loss of the

118 ECM proteins Collagen IV (red), and Perlecan (green), coinciding with the disruptions in
119 Laminin (purple) (Figure 1E). These data suggest that while dystroglycan is not required
120 for the initial formation of the ILM, it is essential for its maturation and maintenance.
121 Furthermore, dystroglycan is critical for the ILM to function as a structural barrier to
122 prevent the ectopic migration of neurons into the vitreous space.

123 The hyaloid vasculature in the embryonic retina normally regresses as the retinal
124 vascular plexus emerges through the optic nerve head beginning around birth (Fruttiger,
125 2007). Previous studies have found that defects in ILM integrity disrupt retinal
126 vasculature development (Edwards et al., 2010; Lee et al., 2005; Takahashi et al., 2011;
127 Tao and Zhang, 2016). In agreement with these findings, we observe that at embryonic
128 ages in *ISPD^{L79*/L79*}* mutant retinas, the hyaloid vasculature becomes embedded within
129 the ectopic retinal neuron layer (Supplemental Figure 2A), and fails to regress at P0
130 (Supplemental Figure 2B). In addition, the emergence of the retinal vasculature is
131 stunted in *ISPD^{L79*/L79*}* mutants (Supplemental Figure 2B). This is likely due to defects in
132 the migration of astrocytes, which also emerge from the optic nerve head just prior to
133 endothelial cells and require an intact ILM for their migration (Tao and Zhang, 2016).

134 We previously showed that the organization of the basement membrane by
135 dystroglycan provides a permissive growth substrate for axons in the developing spinal
136 cord (Wright et al., 2012). In addition, contact with laminin in the ILM stabilizes the
137 leading process of newly generated RGCs to direct the formation of the nascent axon
138 (Randlett et al., 2011). These axons remain in close proximity to the ILM as they extend
139 centrally towards the optic nerve head, forming the OFL. Therefore, we examined
140 whether the disruptions in the ILM affected the guidance of RGC axons in *ISPD^{L79*/L79*}*

141 and *DG^{F/-}*; *Sox2^{cre}* mutants. At e13, axons in both control and mutant retinas formed a
142 dense and continuous network in the basal retina, directly abutting the ILM (Figure 2A).
143 In contrast, at e16 (Figure 2B) and P0 (Figure 2C), RGC axons in *ISPD^{L79*/L79*}* and *DG^{F/-}*
144 ; *Sox2^{cre}* mutants were highly disorganized, exhibiting both defasciculation (asterisks)
145 and hyperfasciculation (arrowheads).

146 To gain further insight into the specific defects that occur in RGC axons, we used a
147 flat mount retina preparation. Regardless of their location in the retina, all RGCs orient
148 and extend their axons towards the center of the retina, where they exit the retina
149 through the optic nerve head (Bao, 2008). In control retinas at e16 (Figure 2D, left
150 panel) and P0 (Figure 2E, left panel) axons traveled towards the optic nerve head in
151 fasciculated, non-overlapping bundles. By e16 RGC axons in both *ISPD^{L79*/L79*}* and
152 *DG^{F/-}*; *Sox2^{cre}* mutants were highly defasciculated and a large proportion frequently
153 grew in random directions without respect to their orientation to the optic nerve head,
154 resulting in their failure to exit the retina. However, it is important to note that some
155 axons retained their appropriate centrally-orientated trajectory, which may be indicative
156 of RGC axons that have already traversed the retina to the optic nerve head prior to the
157 degeneration of the ILM (Figure 1) (Petros et al., 2008). Together, these data show that
158 proper growth and guidance of RGC axons to the optic nerve head requires
159 dystroglycan to maintain an intact ILM as a growth substrate.

160

161 **Dystroglycan is required for axonal targeting, dendritic lamination, and cell**
162 **spacing in the postnatal retina**

163 Our results in *ISPD^{L79*/L79*}* and *DG^{F/-}; Sox2^{cre}* mutants demonstrate that
164 dystroglycan is required for ILM integrity and to prevent the ectopic migration of neurons
165 into the vitreous (Figure 1), consistent with other models of dystroglycanopathy.
166 However, the specific neuronal subtypes affected in models of dystroglycanopathy are
167 unknown, and the role of dystroglycan in regulating postnatal aspects of retinal
168 development has not been examined. The synaptic layers of the retina develop
169 postnatally, with tripartite synapses between the photoreceptors, bipolar cells and
170 horizontal cells forming in the OPL, and synapses between bipolar cells, amacrine cells
171 and retinal ganglion cells forming in the IPL. The development of these synaptic layers
172 requires the precise stratification of both axons and dendrites that occurs between P0
173 and P14. Since *ISPD^{L79*/L79*}* and *DG^{F/-}; Sox2^{cre}* mutant mice exhibit perinatal lethality,
174 we deleted *dystroglycan* selectively from the early neural retina and ventral forebrain
175 using a *Six3^{Cre}* driver (Furuta et al., 2000) (Supplemental Figure 3).

176 We first confirmed that *DG^{F/-}; Six3^{cre}* mice recapitulated the retinal phenotypes
177 identified in *ISPD^{L79*/L79*}* and *DG^{F/-}; Sox2^{cre}* mice. We observed a degeneration of the
178 ILM (laminin, purple) accompanied by ectopic migration of neurons into the vitreous,
179 and abnormal fasciculation and guidance of RGC axons at P0 (Figure 3A-B). While
180 fully penetrant, the ILM degeneration and neuronal migration defects in *DG^{F/-}; Six3^{cre}*
181 mice were milder than in *DG^{F/-}; Sox2^{cre}* mice, exhibiting a patchiness that was
182 distributed across the retina (Supplemental Figure 3C). The defects in *DG^{F/-}; Six3^{cre}*
183 mice contrast the finding that conditional deletion of *dystroglycan* with *Nestin^{cre}* does not
184 affect the overall structure of the retina (Satz et al., 2009). We find that this difference is
185 likely due to the onset and pattern of *Cre* expression, as recombination of a *Cre*-

186 dependent reporter (*Rosa26-lox-stop-lox-TdTomato; Ai9*) occurred earlier and more
187 broadly in *Six3^{Cre}* mice than in *Nestin^{Cre}* mice (Supplemental Figure 3).

188 *DG^{F/-}; Six3^{Cre}* mice are healthy and survive into adulthood, allowing us to examine
189 the role of dystroglycan in postnatal retinal development. We analyzed *DG; Six3^{Cre}*
190 retinas at P14 when migration is complete and the laminar specificity of axons and
191 dendrites has been established (Morgan and Wong, 1995). The overall architecture of
192 the ONL appeared unaffected by the loss of dystroglycan in *DG^{F/-}; Six3^{Cre}* mice, and cell
193 body positioning of photoreceptors appeared similar to controls (Supplemental Figure
194 4). Within the INL, the laminar positioning of rod bipolar cell bodies (PKC, Figure 3C),
195 cone bipolar cell bodies (SCGN, Figure 3D) and horizontal cells (arrows, Calbindin,
196 Figure 3F) and the targeting of their dendrites to the OPL appeared normal in *DG^{F/-};*
197 *Six3^{Cre}* mutants. However, bipolar cell axons that project towards the inner retina and
198 are normally confined to the synaptic layers in the IPL extended aberrant projections
199 into the ectopic clusters (Figure 3C).

200 In contrast, subsets of amacrine and ganglion cells labeled by ChAT (starburst
201 amacrine cells, Figure 3E), calbindin (Figure 3F) calretinin (Figure 3G) that are normally
202 confined to the INL and GCL were present in the ectopic clusters that protrude into the
203 vitreous space. Glycinergic amacrine cells (GlyT1, Figure 3H), whose cell bodies are
204 normally found in a single layer within the INL, were also present within ectopic clusters.
205 Compared to the OPL, which appeared grossly normal, dendritic stratification within the
206 IPL in *DG^{F/-}; Six3^{Cre}* mutant retinas was highly disrupted. The normally tightly laminated
207 dendritic strata appeared expanded (Figure 3E), fragmented (Figure 3E-G) and
208 occasionally lacked an entire lamina (Figure 3F). These defects were restricted to

209 regions of the retina where ectopic neuronal clusters were present, whereas regions of
210 the *DGF^{-/-}; Six3^{cre}* mutant retina with normal cellular migration and lamination also had
211 normal dendritic stratification (Supplemental Figure 3). These results demonstrate that
212 the ectopic clusters consisted of multiple subtypes of amacrine cells and ganglion cells
213 that normally reside in the INL and GCL, and that the disorganization of the dendritic
214 strata are likely secondary to the cell migration defects.

215 Over the course of retinal development, multiple cell types, including horizontal
216 cells and amacrine cells, develop mosaic spacing patterns that ensure cells maintain
217 complete and non-random coverage over the surface of the retina (Wassle and
218 Riemann, 1978). This final mosaic pattern is established by both the removal of excess
219 cells through apoptosis and the lateral dispersion of “like-subtype” cells via homotypic
220 avoidance mechanisms (Kay et al., 2012; Li et al., 2015). To determine whether the
221 defects in establishing proper positioning of retinal subtypes in *DGF^{-/-}; Six3^{cre}* mutants
222 extends to mosaic spacing, we performed nearest neighbor analysis. For horizontal
223 cells, which exhibit normal lamination in *DGF^{-/-}; Six3^{cre}* mutant retinas, we observed a
224 small, but significant reduction in cellular density (Figure 5F). Despite the reduction in
225 the density of horizontal cells, nearest neighbor curves between controls and mutants
226 are the same shape, indicating that horizontal cell mosaics are maintained in
227 dystroglycan mutants (Figure 4A, B, Two-Way ANOVA, $p < 0.01$).

228 ChAT positive starburst amacrine cells are present in two distinct lamina that form
229 mosaic spacing patterns independent from one another. Consistent with this, ChAT
230 labeled cells in the INL showed normal mosaic cell spacing (Figure 4C, top, Figure 4D,
231 top, Two-Way ANOVA, $p > 0.05$). In contrast, the GCL contained prominent ChAT

232 positive clusters that corresponded to the ectopic protrusions that extend into the
233 vitreous, resulting in a decrease in cell spacing as determined by nearest neighbor
234 analysis, (Figure 4C, bottom, Figure 4D, bottom, Two-Way ANOVA, $p < 0.01$). These
235 results demonstrate that laminar migration defects in $DG^{F/-}; Six3^{cre}$ mutants degrade the
236 mosaic spacing of cells in the GCL, and that contact with an intact ILM is likely required
237 for the proper lateral dispersion of these cells.

238

239 **Deletion of dystroglycan leads to a loss of photoreceptors, horizontal cells and** 240 **ganglion cells**

241 During development, normal physiological apoptotic cell death during the first two
242 postnatal weeks plays an important role in retinal maturation (Young, 1984). This
243 process is critical for establishing the proper numbers and spacing of some subtypes of
244 cells across the mature retina, as well as removing cells that fail to connect to
245 appropriate synaptic targets (Braunger et al., 2014). Degeneration of the ILM during
246 development can lead to a reduction in the number of ganglion cells, and previous
247 analysis of dystroglycanopathy mutants has noted thinning of the retina (Chan et al.,
248 2010; Halfter et al., 2005; Lee et al., 2005; Satz et al., 2008; Takahashi et al., 2011). In
249 agreement with these results, we observed that the retinas of $DG^{F/-}; Six3^{cre}$ mutants are
250 thinner (Figure 3, 5). However, the specific cell types affected by the loss of
251 dystroglycan in the retina are unknown.

252 To investigate the mechanism by which loss of dystroglycan contributes to retinal
253 thinning, we began by measuring the distance between the edges of the inner and outer
254 retina in control and $DG^{F/-}; Six3^{cre}$ mutants by DAPI staining and found that there was a

255 significant reduction in overall retinal thickness by approximately 20% in mutants
256 (Figure 5A, blue, Figure 5B, t test, $p < 0.01$). We next investigated which specific cell
257 types contribute to retinal thinning. In the outer retina, the thickness of the photoreceptor
258 layer (recoverin, Figure 5A, green, Figure 5C, t-test, $p < 0.05$) was reduced by
259 approximately 20% and the density of horizontal cells had a small, yet significant
260 reduction in $DG^{F/-}; Six3^{cre}$ mutants (calbindin, Figure 5F, t-test, $p < 0.05$). In contrast, the
261 thickness of the bipolar cell layer (Chx10, Figure 5A, purple, Figure 5D, t-test, $p < 0.05$)
262 was normal. In the inner retina, there was a 50% reduction in the density of ganglion
263 cells (Figure 5G, H, t-test, $p < 0.0001$), while the density of ChAT+ starburst amacrine
264 cells in both the GCL and INL was normal in $DG^{F/-}; Six3^{cre}$ mutants (Figure 5E, t-test,
265 $p < 0.05$). Thus, the loss of photoreceptors, horizontal cells and RGCs contribute to the
266 overall thinning of the retina.

267 To determine whether the reduction in photoreceptors, horizontal cells and RGCs in
268 the absence of dystroglycan was the result of increased cell death, we examined early
269 postnatal ages when normal physiological apoptosis occurs in the retina. In $DG^{F/-};$
270 $Six3^{cre}$ mutants at P0, we observed an increased number of cleaved caspase-3 positive
271 cells that was restricted to the ganglion cell layer (Figure 5I, J, t-test, $p < 0.05$) and was
272 not observed in other layers of the retina (data not shown). We also examined
273 $ISPD^{L79*/L79*}$ mutants to assess GCL apoptosis in a dystroglycanopathy model. Prior to
274 the normal period of physiological apoptosis in the retina we observed a massive
275 increase in caspase-3 positive cells at e16 in mutants (Figure 5J t-test, $p < 0.0001$) that
276 continued through P0 (Figure 5I, J, t-test, $p < 0.0001$). These results led us to conclude

277 that the dramatic loss of RGCs in $DG^{F/-}; Six3^{cre}$ mutants is due to increased apoptotic
278 cell death.

279

280 **Dystroglycan functions non-cell autonomously as a scaffold in the developing** 281 **retina**

282 We next sought to provide mechanistic insight into how dystroglycan regulates
283 retinal development *in vivo*. In the cerebral cortex, the loss of dystroglycan results in
284 breaches of the pial basement membrane and detachment of neuroepithelial endfeet
285 from the pial surface, depriving neurons of a migratory scaffold. In addition, the cortical
286 basement membrane defects cause the mis-positioning of Cajal-Retzius cells, which are
287 the source of Reelin that regulates somal translocation of neurons as they detach from
288 the neuroepithelial scaffold (Nakagawa et al., 2015). Deletion of *dystroglycan*
289 specifically from postmitotic neurons does not result in a migration phenotype (Satz et
290 al., 2010), supporting a model in which the cortical migration phenotypes arise due to
291 disrupted interactions between the basement membrane and neuroepithelial scaffold. In
292 contrast to the cerebral cortex, the basal migration of RGCs does not involve contact
293 with the neuroepithelial scaffold. Instead, newly born RGCs migrate via somal
294 translocation using an ILM-attached basal process that eventually becomes the nascent
295 axon (Icha et al., 2016; Randlett et al., 2011). Dystroglycan's expression in RGCs
296 (Montanaro et al., 1995), and the restriction of neuronal migration and axon guidance
297 defects to the GCL raise the possibility that dystroglycan could be functioning cell-
298 autonomously in the basal processes of newly born RGCs. To test this possibility, we
299 generated $DG^{F/-}; Islet1^{cre}$ conditional knockouts. *Islet1* is expressed in the majority of

300 ganglion cells as they differentiate from the retinal progenitor pool (Pan et al., 2008).
301 Analysis of *Isl1^{cre}* mice at e13 confirmed recombination occurs in the majority of newly
302 born ganglion cells, but not in neuroepithelial progenitors (Supplemental Figure 5).
303 Examination of *DG^{F/-}; Isl1^{cre}* mutants indicated that deletion of *dystroglycan* selectively
304 from RGCs did not affect ILM integrity (Figure 6A, middle panel). Neuronal migration
305 (Figure 6A, C and D, middle panels), axon guidance (Figure 6A and B, middle panels)
306 and the stratification of dendrites in the IPL (Figures 6 C-D, middle panels) all appeared
307 normal in *DG^{F/-}; Isl1^{cre}* mutants. These results demonstrate that dystroglycan is not
308 required within RGCs themselves during retinal development.

309 Dystroglycan consists of two subunits that play distinct roles in the overall function
310 of the protein. The extracellular α -subunit is heavily glycosylated and functions as an
311 extracellular scaffold by binding to extracellular matrix components such as laminin. The
312 β -subunit contains a transmembrane and intracellular domain, and can bind directly to
313 dystrophin and other modifiers of the actin cytoskeleton as well as initiate intracellular
314 signaling cascades (Moore and Winder, 2010). The intracellular domain of dystroglycan
315 is required for the localization of dystrophin to the ILM, and mice lacking the intracellular
316 domain of dystroglycan (*DG^{- β cyt}*) (Satz et al., 2009) or the predominant retinal isoform of
317 dystrophin (*Mdx^{3Cv}*) (Blank et al., 1999) have abnormal scotopic electroretinograms,
318 suggesting a defect in retinal function. While these mice do not have any disruptions in
319 the ILM or gross malformations in the retina, whether dystroglycan signaling through
320 dystrophin is required for neuronal migration, axon guidance or dendritic stratification
321 has not been examined. Consistent with the original report, examination of the ILM and
322 overall architecture of the retina is normal in *DG^{- β cyt}* mice. In addition, we find that

323 neuronal migration, axon guidance and stratification of dendritic lamina are unaffected
324 in *DG^{-/βcyt}* mice (Figure 6A-D, right panel). Therefore, intracellular signaling, including
325 through dystrophin, is not required for these aspects of retinal development. Taken
326 together with our results in *DG^{F/-}; Isl1^{cre}* mutants, these findings indicate that
327 dystroglycan primarily functions in neuroepithelial cells as an extracellular scaffold to
328 regulate the structural integrity of the ILM. The progressive degeneration of the ILM then
329 leads to secondary defects including aberrant migration, axon guidance and dendritic
330 stratification that primarily affect the inner retina.

331

332 **Dystroglycan is dispensable for the generation of spontaneous retinal waves**

333 One of the critical functions for laminar targeting in neural circuit development is to
334 ensure that the axons and dendrites of appropriate cell types are in physical proximity to
335 one another during synaptogenesis. In addition to regulating the laminar positioning of
336 neurons in the cortex and retina, dystroglycan is required for the development of a
337 subset of inhibitory synapses in the brain (Fruh et al., 2016). Therefore, we investigated
338 the possibility that the loss of dystroglycan disrupts synapse formation in the retina.
339 Previous studies have shown that ribbon synapses in the OPL are dysfunctional in the
340 absence of dystroglycan or its ligand pikachurin (Sato et al., 2008). These synapses are
341 normal at the resolution of light microscopy, but electron microscopy reveals that
342 dystroglycan and pikachurin are required for the insertion of bipolar cell dendrite tips
343 into ribbon synapse invaginations (Omori et al., 2012). Consistent with these results, we
344 found that pre- and post-synaptic markers for ribbon synapses appear normal at the
345 resolution of light microscopy (Figure 7A). In the inner retina, markers for excitatory

346 synapses (VGLUT1, Figure 7B) and inhibitory synapses (VGAT, Figure 7C) were
347 present in the IPL, but were also present in the mis-localized ectopic cell clusters that
348 protrude into the vitreous (asterisks). This finding is similar to a recent study in which
349 mice lacking the Cas family of intracellular adaptor proteins express synaptic markers
350 localized to aberrant neuronal ectopia that protrude into the vitreous (Riccomagno et al.,
351 2014). Therefore, these results suggest that mis-laminated neurons in the retina are
352 still able to recruit synaptic partners, despite their abnormal location.

353 The presence of synaptic markers in ectopic neuronal clusters in the inner retina
354 does not guarantee normal function of these neurons. Recording synaptic activity in
355 RGCs in response to light stimuli in *DG^{F/-}; Six3^{cre}* mutants is not feasible due the
356 requirement for dystroglycan at photoreceptor ribbon synapses. We instead analyzed
357 retinal waves, which are spontaneous bursts of activity that propagate across the retina
358 prior to eye opening and are independent of light stimulation. During early postnatal
359 development, these waves are initiated by acetylcholine (ACh) release from starburst
360 amacrine cells and propagate along the starburst amacrine cell network prior to
361 transmission to RGCs (Xu et al., 2016). In *DG^{F/-}; Six3^{cre}* mutants, ChAT positive
362 starburst amacrine cells are present in normal numbers, and while they are normally
363 localized and mosaically spaced in the INL, they are profoundly disorganized in the
364 GCL. Therefore, we expected that these defects might affect the propagation of retinal
365 waves through the starburst amacrine cell and RGC network. As disruptions in the ILM
366 in *DG^{F/-}; Six3^{cre}* mutants would lead to unequal loading of cell permeable calcium
367 indicators, we utilized the genetically-encoded calcium indicator GCaMP6f crossed onto
368 the *DG; Six3^{cre}* line to visualize retinal waves.

369 Retinal waves in control *DG^{F/+}; Six3^{cre}; R26-LSL-GCaMP6f* retinas at P1-P2 were
370 robust and had similar spatiotemporal features (size, rate of propagation, refractory
371 period) to waves measured using cell-permeable calcium indicators (Arroyo and Feller,
372 2016). Consistent with previous reports, there is a broad distribution of wave size in
373 control retinas (Figures 8A, 8C). Neighboring waves do not overlap with one another,
374 but rather tile the retinal surface during the two-minute imaging period. To our surprise,
375 retinal waves were present and appeared grossly normal in *DG^{F/-}; Six3^{cre}; R26-LSL-*
376 *GCaMP6f* mutants (Figure 8B, D). Waves in control and mutant retinas exhibited a
377 similar distribution in wave size (Figure 8 E, F), and the average wave size showed no
378 statistical difference. The rate of wave propagation showed a similar distribution
379 between controls and mutants. The average rate of wave propagation showed a small,
380 but statistically significant, decrease (Wilcoxon Rank Sum test, $p < 0.05$). Thus, despite
381 the dramatic disorganization of ChAT positive starburst amacrine cells in the GCL of
382 *DG^{F/-}; Six3^{cre}* mutants, the generation and propagation of retinal waves persisted.

383

384 **Discussion**

385

386 Defects in retinal structure and function are commonly observed in human patients
387 with dystroglycanopathy, and are recapitulated in mouse models of dystroglycanopathy
388 (Chan et al., 2010; Lee et al., 2005; Satz et al., 2008; Satz et al., 2009; Takahashi et al.,
389 2011; Takeda et al., 2003). However, the mechanism of dystroglycan function in the
390 retina and the consequence of its loss on specific cell types are poorly understood. Our
391 study establishes a critical role for dystroglycan in regulating neuronal migration in order
392 to establish laminar architecture and mosaic spacing in the inner retina. In the absence

393 of functional dystroglycan, the retinal ILM undergoes rapid and progressive
394 degeneration, leading to the formation of cellular ectopias in the vitreous space and
395 defects in intraretinal axon guidance. In the postnatal retina, these migration defects
396 result in the mis-localization of multiple subtypes of GCL and INL cells into cellular
397 ectopias and disrupt the mosaic spacing of cells in the GCL. Mechanistically, we show
398 that these defects are exclusively due to dystroglycan's function as an extracellular
399 scaffold, as mice lacking the intracellular domain of dystroglycan ($DG^{-/\beta\text{cyt}}$) appear
400 phenotypically normal. Furthermore, dystroglycan functions non-cell autonomously, as
401 selective deletion of *dystroglycan* from postmitotic RGCs ($DG; Isl1^{\text{cre}}$) did not affect ILM
402 integrity, neuronal migration or axon guidance. Despite the dramatic disruptions in
403 cellular lamination in the GCL and dendritic stratification in the IPL in $DG; Six3^{\text{cre}}$
404 mutants, dystroglycan appears dispensable for the formation of synapses and the
405 generation of spontaneous, light-independent activity in the retina.

406

407 **Temporal requirement for dystroglycan during retinal development.**

408 Using two genetic models for the complete loss of functional dystroglycan ($ISPD^{\text{L79*}}$
409 and $DG; Sox2^{\text{Cre}}$), we demonstrated that after the ILM forms, it rapidly degenerates in
410 the absence of dystroglycan. In $DG; Six3^{\text{cre}}$ mutants, in which broad recombination
411 occurs throughout the retina by e13, a milder degeneration of the ILM occurs. In
412 contrast, the ILM appears grossly normal in $DG; Nestin^{\text{cre}}$ mutants in which broad
413 recombination does not occur until later stages (Satz et al., 2009) (Supplemental Figure
414 3). These results suggest that dystroglycan is not required for the formation of the

415 nascent ILM, but rather plays a critical, yet transient, role in maintaining ILM structure as
416 it expands to accommodate the growing retina.

417 Recruitment of laminin is a critical early step in the assembly of the ILM, and several
418 laminin mutants have disruptions in ILM integrity (Edwards et al., 2010; Gnanaguru et
419 al., 2013; Pinzon-Duarte et al., 2010). The localization of laminin to the early ILM even
420 in the complete absence of dystroglycan raises the possibility that other laminin
421 receptors, such as β -1 Integrin, may compensate for the loss of dystroglycan. Mice
422 lacking β -1 Integrin in the retina exhibit a similar defect to *dystroglycan* mutants, with
423 normal ILM formation followed by rapid degeneration, supporting the possibility of
424 redundancy between dystroglycan and β -1 Integrin (Riccomagno et al., 2014).
425 Surprisingly however, mice in which both dystroglycan and β -1 Integrin are deleted from
426 the retina (*DG; ItgB1; Six3^{Cre}*) still formed an ILM, and exhibited similar phenotypic
427 severity to *DG; Six3^{Cre}* mutant retinas (unpublished observations). These results
428 demonstrate that both dystroglycan and β -1 Integrin are dispensable, and sulfated
429 glycolipids alone are likely sufficient for the recruitment of laminin during the initial
430 formation of the ILM.

431

432 **The ILM is required for neuronal migration in the retina**

433 The role of dystroglycan has been extensively studied in the developing cortex,
434 where it regulates the attachment of the radial glial endfeet to the pial basement
435 membrane (Myshra et al., 2012). The degeneration of the radial glia processes and the
436 ectopic clustering of Cajal-Retzius neurons, the primary source of reelin in the
437 developing cortex, are the earliest observable pathological features in models of

438 dystroglycanopathy (Booler et al., 2016; Nakagawa et al., 2015). The loss of a radial
439 migration scaffold and the abnormal distribution of reelin are thought to be the principal
440 drivers of structural brain defects in dystroglycanopathy. In contrast to the cortex, birth
441 order does not predict the laminar positioning of retinal neurons, retinal neuron
442 migration does not involve contact with the neuroepithelial scaffold, and there is no cue
443 analogous to reelin to signal the termination retinal neuron migration. Therefore, while
444 our results demonstrate that dystroglycan functions primarily in neuroepithelial cells in
445 the retina, the functional implications are distinct from its role in cortical neuroepithelial
446 cells.

447 We find that while dystroglycan is required to establish the proper architecture of the
448 retina, it appears that only amacrine cells and RGCs are affected. What is the driving
449 force behind the selective localization of amacrine cells and RGCs to the ectopic
450 clusters that protrude into the vitreous? Previous work has shown that elimination of
451 RGCs does not dramatically affect the lamination of other retinal neurons or the overall
452 architecture of the retina (Kay et al., 2004; Wang et al., 2001). However, if RGCs are
453 selectively mis-localized, other retinal neurons will organize themselves around the
454 displaced RGCs, resulting in an overall disorganization of retinal lamination (Icha et al.,
455 2016). In *dystroglycan* mutants, RGCs are the first neurons to encounter the
456 degenerating ILM and inappropriately migrate into the vitreous. Mis-localized RGCs
457 may then act actively recruit later born neurons such as amacrine cells to inappropriate
458 locations. Consistent with previous results observed in β -1 Integrin mutants, synaptic
459 markers were present in ectopic clusters, suggesting that neurons retain the ability to
460 recruit synaptic partners despite their inappropriate location (Riccomagno et al., 2014).

461 Many neurons migrate radially to their appropriate lamina, then undergo tangential
462 migration to establish non-random mosaic patterns (Galli-Resta et al., 1997; Reese et
463 al., 1999). This tangential migration involves interactions between immature neurites of
464 neighboring cells (Galli-Resta et al., 2002; Huckfeldt et al., 2009) and short-range
465 interactions mediated by DSCAM and MEGF10/11 (Fuerst et al., 2008; Kay et al.,
466 2012). A key feature of this process is that it occurs between homotypic cells within the
467 same lamina, and cells in which mosaic spacing is disrupted are no longer restricted to
468 a two-dimensional plane. In *dystroglycan* mutants, the mosaic spacing of horizontal
469 cells and INL starburst amacrine cells is normal, but is dramatically disrupted in
470 starburst amacrine cells in the GCL. This defect is not due to dystroglycan functioning
471 within starburst amacrine cells, as mosaic spacing was normal in *DG; Isl1^{Cre}* mutant
472 retinas (data not shown). Rather, the selective defects in mosaic spacing of GCL
473 starburst amacrine cells suggests that this may be a consequence of disrupting the two-
474 dimensional organization of the GCL. Alternatively, mosaic spacing of cells within the
475 GCL may require cues present in the ILM to guide tangential dispersion.

476

477 **Intraretinal axon growth and guidance requires an intact ILM**

478 Previous work has shown that the ILM and other basement membranes function as
479 excellent growth substrates for extending axons (Halfter et al., 1987; Wright et al.,
480 2012). Basement membranes are highly dynamic structures that not only contain pro-
481 growth ECM molecules such as laminins and collagens, but also regulate the
482 distribution of secreted axon guidance cues in the extracellular environment (Chai and
483 Morris, 1999; Wright et al., 2012; Xiao et al., 2011). A number of secreted cues direct

484 intraretinal axon guidance of RGCs. Deletion of Netrin (Deiner et al., 1997) specifically
485 affects exit of RGC axons through the optic nerve head, and deletion of Slits (Thompson
486 et al., 2006) or Sfrps (Nieto-lopez et al., 2015) leads to the invasion of RGC axons into
487 the outer retina. These specific phenotypes are distinct from those we observed in the
488 absence of dystroglycan. The randomized growth and defasciculation of axons we
489 observed in *ISPD^{L79*}* and *DG; Six3^{Cre}* mutant retinas is more consistent with defects
490 observed upon deletion of adhesion receptors such as L1 (Bastmeyer et al., 1995),
491 NCAM (Brittis et al., 1995) or DM-GRASP (Ott et al., 1998). These results suggest that
492 the role of dystroglycan in guiding axons along the ILM is primarily to regulate axonal
493 adhesion. While there are extensive intraretinal axon guidance defects in the absence
494 of dystroglycan, some axons still appear normally oriented and fasciculated, exit the
495 optic nerve head and project to the optic chiasm (Figure 2, unpublished results). We
496 hypothesize that these normally oriented axons emanate from early born RGCs that
497 begin to extend their axons as early as e13, prior the degeneration of the ILM. In
498 contrast, later born RGCs that initiate axon growth after ILM degeneration lack an
499 appropriate growth substrate and fail to orient their axons to the optic nerve head.

500

501 **Loss of RGCs, photoreceptors and horizontal cells in the absence of** 502 **dystroglycan**

503 Previous studies of mouse models of dystroglycanopathy have consistently noted
504 retinal thinning. However, based on these studies, it was unclear which retinal cell types
505 were affected. Our comprehensive analysis of P14 *DG; Six3^{cre}* mutant retinas found that
506 bipolar layer thickness was normal and INL and GCL starburst amacrine cells were

507 present at normal numbers. In contrast, photoreceptor layer thickness was reduced by
508 approximately 20%, horizontal cell number in the INL was reduced by 16%, and RGC
509 number exhibited a dramatic 50% reduction (Figure 5).

510 Analysis of e16 and P0 retinas from *ISPD^{L79*}* and *DG; Six3^{cre}* mutants indicated that
511 the loss of RGCs was due to increased apoptosis of cells in the GCL that preceded and
512 extended into the normal window of developmental apoptotic cell death. This increase
513 in apoptotic cell death did not persist in adult (P56) *DG; Six3^{cre}* mutants (data not
514 shown), suggesting it was likely restricted to the developing retina. Why are RGCs
515 selectively lost at such a high rate in *DG; Six3^{cre}* mutants? One possibility is that the
516 degeneration of the ILM selectively affects cells in the ganglion cell layer (ganglion cells
517 and displaced amacrine cells). However, amacrine cell number remained unchanged in
518 the GCL. Another possibility is that RGCs are selectively affected since they are the
519 only cell type to project out of the retina. Indeed, we observed profound defects in the
520 ability of RGC axons to navigate the optic chiasm in *ISPD^{L79*}* and *DG; Six3^{cre}* mutants
521 (unpublished observations). These results suggest that the failure to reach
522 retinorecipient regions of the brain resulted in the death of RGCs. It was originally
523 postulated that BDNF from retinorecipient regions of the brain signaling through the
524 TrkB receptor on RGCs regulates the survival of RGCs during development. However,
525 RGC survival is unaffected in TrkB and BDNF knockouts (Cellerino et al., 1997; Rohrer
526 et al., 2001). Therefore, while our data is consistent with the need for target-derived
527 factors to support the survival of RGCs during development, the identity of these
528 molecules remains elusive.

529 We also observed a reduction in thickness of the photoreceptor layer and in the
530 number of horizontal cells in *DG; Six3^{cre}* mutants. While we did not observe increased
531 caspase-3 reactivity in these cells at P0, it is possible that the loss of cells occurred
532 gradually during the first two postnatal weeks. Dystroglycan is required for the proper
533 formation of ribbon synapses between photoreceptors, horizontal cells and bipolar cells
534 in the OPL (Omori et al., 2012; Sato et al., 2008). Therefore, the loss of appropriate
535 synaptic contact in the absence of dystroglycan may lead to the elimination of a
536 proportion of photoreceptors and horizontal cells.

537

538 **Persistence of retinal waves in the absence of dystroglycan**

539 The profound defects in lamination and dendritic stratification of ChAT positive
540 starburst amacrine cells in *DG; Six3^{cre}* mutants led us to hypothesize that this would
541 affect their ability to generate retinal waves. These waves are initiated by the
542 spontaneous activity of starburst amacrine cells, independent of light stimuli, allowing us
543 to circumvent the requirement for dystroglycan in proper transmission at ribbon
544 synapses. Contrary to our expectations, retinal waves were present and propagated
545 normally in *DG; Six3^{cre}* mutants (Figure 8). The persistence of retinal waves even in the
546 context of disrupted starburst amacrine cell organization supports the model that these
547 waves are the product of volume release of ACh from starburst amacrine cells that can
548 trigger extra-synaptic responses (Ford et al., 2012). Using a cell-based sensor, Ford
549 and colleagues detected ACh release several micrometers above the surface of the
550 retina, suggesting that ACh diffusion is sufficient to trigger a response in cells that are
551 not physically connected. Therefore, the relatively normal organization of INL starburst

552 amacrine cells may be sufficient to overcome the disorganization of GCL starburst
553 amacrine cells. We did observe a slight reduction in the rate of wave propagation, which
554 may be due to the reduced density of cells with calcium transients within a retinal wave
555 that were observed in *DG; Six3^{cre}* mutants. This reduced density likely reflects the
556 nearly 50% reduction in ganglion cell number, and suggests that while a full
557 complement of RGCs is not required for the propagation of retina waves, it may affect
558 their rate of propagation. While our results demonstrate that synaptic markers are
559 present in the inner retina and spontaneous retinal activity persists in *DG; Six3^{cre}*
560 mutants, it remains unknown whether synaptic transmission between specific cell types
561 within the inner retina is affected by the absence of dystroglycan.

562 Taken together, our data demonstrate that dystroglycan is required for multiple
563 aspects of retinal development. Similar to its role in the cortex, dystroglycan in the
564 retina functions within neuroepithelial cells to regulate the structural integrity of a
565 basement membrane (the ILM), which is required for the coordination of neuronal
566 migration, axon guidance and dendritic stratification in the inner retina. Overall, our data
567 suggest that the disorganization of the inner retina and the loss of photoreceptors,
568 horizontal cells and RGCs are key contributors to visual impairment in
569 dystroglycanopathy.

570

571 **Experimental Procedures**

572

573 **Animals**

574 Animal procedures were approved by OHSU Institutional Animal Care and Use
575 Committee and conformed to the National Institutes of Health *Guide for the care and*

576 *use of laboratory animals*. Animals were euthanized by administration of CO₂. The day
577 of vaginal plug observation was designated as embryonic day 0 (e0) and the day of birth
578 in this study was designated as postnatal day 0 (P0). The generation and genotyping
579 protocols for *ISPD^{L79*/L79*}* (Wright et al., 2012), *DG^{F/F}* (Moore et al., 2002) and *DG^{βcyt}*
580 (Satz et al., 2009) mice have been described previously. The presence of the cre allele
581 in *Six3^{Cre}* (Furuta et al., 2000), *Isl1^{Cre}* (Yang et al., 2006) and *Nestin^{Cre}* mice (Tronche et
582 al., 1999) was detected by generic cre primers. *ISPD^{+/L79*}*, *DG^{ββ/+}*, and *DG^{F/+}*; *Six3^{Cre}* or
583 *DG^{F/+}* age matched littermates were used as controls.

584 **Tissue Preparation and Immunohistochemistry**

585 Embryonic retinas were left in the head and fixed overnight at 4°C in 4% PFA and
586 washed in PBS for 30 minutes. Heads were equilibrated in 15% sucrose overnight and
587 flash frozen in OCT medium. Postnatal retinas were dissected out of the animal and the
588 lens was removed from the eyecup. Intact retinas were fixed at room temperature for 30
589 minutes in 4% PFA. Retinas were washed in PBS for 30 minutes and equilibrated in a
590 sequential gradient of 10%, sucrose, 20% sucrose and 30% sucrose overnight. Tissue
591 was sectioned on a cryostat at 16-25um. Tissue sections were blocked in a PBS
592 solution containing 2% Normal Donkey Serum and 0.2% Triton for 30 minutes, and
593 incubated in primary antibody overnight at 4°C. Sections were washed for 30 minutes
594 and incubated in secondary antibody in a PBS solution containing 2% Normal Donkey
595 Serum for 2-4 hours. Sections were incubated in DAPI to stain nuclei for 10 minutes,
596 washed for 30 minutes, and mounted using Fluoromount medium. All
597 immunohistochemistry images have n≥3 from at least two different litters of mice. The

598 source and concentration of all antibodies utilized in this study are listed in
599 Supplemental Table 1.

600 **Wholemout retinal staining**

601 Postnatal retinas were dissected out of the animal and the lens was removed from the
602 eyecup. Intact retinas were fixed at room temperature for 30 minutes in 4% PFA.
603 Retinas were incubated in primary antibody diluted in PBS solution containing 2%
604 Normal Donkey Serum and 0.2% Triton for two days at 4°C. Retinas were washed in
605 PBS for one day and incubated in secondary antibody diluted in PBS solution containing
606 2% Normal Donkey Serum for two days at 4°C, washed for one day in PBS and
607 mounted using Fluoromount medium.

608 **Microscopy**

609 Imaging was performed on a Zeiss Axio Imager M2 upright microscope equipped with
610 an ApoTome.2. Imaging of synapses was performed on a Zeiss Elyra PS.1 with LSM
611 710 laser-scanning confocal Super-Resolution Microscope with AiryScan. Imaging of
612 retinal waves was performed on a Nikon TiE inverted microscope with full environmental
613 chamber equipped with a Yokogawa CSU-W1 spinning disk confocal unit.

614 **Quantification of cell number and mosaic spacing**

615 For each experiment, 3-4 locations per retina at the midpoint of each lobe were
616 sampled. Cell counts of horizontal cells (Calbindin), apoptotic cells (Cleaved Caspase-3,
617 P0), and starburst amacrine cells (ChAT) were obtained from 500 x 500 μm images and
618 quantified in FIJI. Cell counts of apoptotic cells (Cleaved Caspase-3, e16) and ganglion
619 cells (RPBMS) were obtained from 250 x 250 μm images and quantified in FIJI.
620 Analysis of retinal mosaics (Calbindin, ChAT) were conducted on 500 x 500 μm images

621 by measuring the X-Y coordinates for each cell and Veronoi domains were calculated in
622 Fiji and nearest neighbor measurements calculated with WinDRP.

623 **Live cell imaging and analysis**

624 Retinas from P1 *DG^{F/+}; Six3^{cre}; R26-LSL-GCaMP6f* and *DG^{F/-}; Six3^{cre}; R26-LSL-*
625 *GCaMP6f* were dissected into chilled Ames' Medium (Sigma) buffered with sodium
626 bicarbonate and bubbled with carbogen gas (95% O₂, 5% CO₂). The retinas were
627 dissected out of the eyecup, mounted RGC side up on cellulose membrane filters
628 (Millipore) and placed in a glass-bottom petri dish containing Ames' Medium. A platinum
629 harp was used to stabilize the filter paper during imaging. Imaging was performed at
630 30°C using a 10x0.45 Plan Apo Air objective with a field of 1664 by 1404 μm with a 3Hz
631 imaging timeframe. The field was illuminated with a 488 nm laser. 3-4 retinal fields were
632 imaged per retina, and each field of retina was imaged for a two-minute time series
633 using a 300ms exposure and each field was sampled 3-5 times per imaging session.

634 Thirty representative control and thirty representative mutant time series were randomly
635 selected for analysis. Only waves that initiated and terminated within the imaging field
636 were used for analysis. To measure wave area, movies were manually viewed using
637 FIJI frame by frame to determine the start and end frame of a wave. A Z-Projection for
638 maximum intensity was used to create an image with the entire wave, and the boundary
639 of the wave was manually traced to determine the area. Wave area per time was
640 calculated by dividing the area of the wave by the duration in seconds of the wave. Any
641 wave lasting less than 2 seconds was not used in analysis, consistent with previous
642 studies (Blankenship et al., 2009).

643 **Statistics**

644 Statistical analysis was performed using JMP Pro 13.0 software (SAS Institute).
645 Comparison between two groups was analyzed using a Student's t-test. Comparison
646 between two or more groups was analyzed using a Two-Way ANOVA and Tukey post-
647 hoc test. Comparison of retinal wave parameters was analyzed using a Wilcoxon Rank
648 Sums test. The significance threshold was set at 0.05 for all statistical tests. * indicates
649 $p < 0.05$; ** indicates $p < 0.01$; *** indicates $p < 0.001$.

650

651 **Acknowledgements**

652 We thank Patrick Kerstein and Kylee Rosette for their technical assistance; Marla Feller
653 and Franklin Caval-Holme for advice on visualizing and analyzing retinal waves; W.
654 Rowland Taylor and Teresa Puthussery and members of their labs for antibodies and
655 technical advice; David Pow for the GlyT1 antibody; Catherine Morgans for the mGluR6
656 antibody, Stefanie Kaech Petrie and the OHSU Advanced Light Microscopy Core (ALM)
657 for assistance with confocal imaging; Alex Kolodkin, Martin Riccomagno, Randall Hand
658 and members of the Campbell and Wright laboratories for discussion throughout the
659 course of this study and comments on the manuscript. This work was supported by NIH
660 Grants R01-NS091027 (K.M.W.), The Medical Research Foundation of Oregon
661 (K.M.W.), NSF GRFP (R.C.), LaCroute Neurobiology of Disease Fellowship (R.C.),
662 Tartar Trust Fellowship (R.C.), NINDS P30-NS061800 (OHSU ALM), and a Paul D.
663 Wellstone Muscular Dystrophy Cooperative Research Center grant to K.P.C.
664 (1U54NS053672). K.P.C. is an investigator of the Howard Hughes Medical Institute

References

Arroyo, D.A., and Feller, M.B. (2016). Spatiotemporal Features of Retinal Waves Instruct the Wiring of the Visual Circuitry. *Front Neural Circuits* 10, 54. PMC4960261. 10.3389/fncir.2016.00054

Bao, Z.Z. (2008). Intraretinal projection of retinal ganglion cell axons as a model system for studying axon navigation. *Brain Research* 1192, 165-177. 10.1016/j.brainres.2007.01.116

Bassett, E.A., and Wallace, V.A. (2012). Cell fate determination in the vertebrate retina. *Trends in neurosciences* 35, 565-573. 10.1016/j.tins.2012.05.004

Bastmeyer, M., Ott, H., Leppert, C.A., and Stuermer, C.A. (1995). Fish E587 glycoprotein, a member of the L1 family of cell adhesion molecules, participates in axonal fasciculation and the age-related order of ganglion cell axons in the goldfish retina. *J Cell Biol* 130, 969-976. PMC2199948

Blank, M., Koulen, P., Blake, D.J., and Kroger, S. (1999). Dystrophin and beta-dystroglycan in photoreceptor terminals from normal and mdx3Cv mouse retinae. *Eur J Neurosci* 11, 2121-2133

Blankenship, A.G., Ford, K.J., Johnson, J., Seal, R.P., Edwards, R.H., Copenhagen, D.R., and Feller, M.B. (2009). Synaptic and extrasynaptic factors governing glutamatergic retinal waves. *Neuron* 62, 230-241. PMC2807181. 10.1016/j.neuron.2009.03.015

Booler, H.S., Williams, J.L., Hopkinson, M., and Brown, S.C. (2016). Degree of Cajal-Retzius Cell Mislocalization Correlates with the Severity of Structural Brain Defects in Mouse Models of Dystroglycanopathy. *Brain Pathology* 26, 465-478. 10.1111/bpa.12306

Braunger, B.M., Demmer, C., and Tamm, E.R. (2014). Programmed cell death during retinal development of the mouse eye. *Adv Exp Med Biol* 801, 9-13. 10.1007/978-1-4614-3209-8_2

Brittis, P.A., Lemmon, V., Rutishauser, U., and Silver, J. (1995). Unique changes of ganglion cell growth cone behavior following cell adhesion molecule perturbations: a time-lapse study of the living retina. *Mol Cell Neurosci* 6, 433-449. 10.1006/mcne.1995.1032

Cellerino, A., Carroll, P., Thoenen, H., and Barde, Y.A. (1997). Reduced size of retinal ganglion cell axons and hypomyelination in mice lacking brain-derived neurotrophic factor. *Mol Cell Neurosci* 9, 397-408. 10.1006/mcne.1997.0641

Chai, L., and Morris, J.E. (1999). Heparan sulfate in the inner limiting membrane of embryonic chicken retina binds basic fibroblast growth factor to promote axonal outgrowth. *Exp Neurol* 160, 175-185. 10.1006/exnr.1999.7195

Chan, Y.M., Keramaris-Vrantsis, E., Lidov, H.G., Norton, J.H., Zinchenko, N., Gruber, H.E., Thresher, R., Blake, D.J., Ashar, J., Rosenfeld, J., *et al.* (2010). Fukutin-related protein is essential for mouse muscle, brain and eye development and mutation recapitulates the wide clinical spectrums of dystroglycanopathies. *Hum Mol Genet* *19*, 3995-4006. 10.1093/hmg/ddq314

Deiner, M.S., Kennedy, T.E., Fazeli, A., Serafini, T., Tessier-Lavigne, M., and Sretavan, D.W. (1997). Netrin-1 and DCC mediate axon guidance locally at the optic disc: loss of function leads to optic nerve hypoplasia. *Neuron* *19*, 575-589

Dobyns, W.B., Pagon, R.A., Armstrong, D., Curry, C.J., Greenberg, F., Grix, A., Holmes, L.B., Laxova, R., Michels, V.V., Robinow, M., *et al.* (1989). Diagnostic criteria for Walker-Warburg syndrome. *Am J Med Genet* *32*, 195-210. 10.1002/ajmg.1320320213

Edwards, M.M., Mammadova-Bach, E., Alpy, F., Klein, A., Hicks, W.L., Roux, M., Simon-Assmann, P., Smith, R.S., Orend, G., Wu, J., *et al.* (2010). Mutations in Lama1 disrupt retinal vascular development and inner limiting membrane formation. *J Biol Chem* *285*, 7697-7711. PMC2844215. 10.1074/jbc.M109.069575

Ford, K.J., Felix, A.L., and Feller, M.B. (2012). Cellular mechanisms underlying spatiotemporal features of cholinergic retinal waves. *The Journal of Neuroscience* *32*, 850-863. PMC3311224. 10.1523/JNEUROSCI.5309-12.2012

Fruh, S., Romanos, J., Panzanelli, P., Burgisser, D., Tyagarajan, S.K., Campbell, K.P., Santello, M., and Fritschy, J.M. (2016). Neuronal Dystroglycan Is Necessary for Formation and Maintenance of Functional CCK-Positive Basket Cell Terminals on Pyramidal Cells. *The Journal of Neuroscience* *36*, 10296-10313. 10.1523/jneurosci.1823-16.2016

Fruttiger, M. (2007). Development of the retinal vasculature. *Angiogenesis* *10*, 77-88. 10.1007/s10456-007-9065-1

Fuerst, P.G., Koizumi, A., Masland, R.H., and Burgess, R.W. (2008). Neurite arborization and mosaic spacing in the mouse retina require DSCAM. *Nature* *451*, 470-474. PMC2259282. 10.1038/nature06514

Furuta, Y., Lagutin, O., Hogan, B.L., and Oliver, G.C. (2000). Retina- and ventral forebrain-specific Cre recombinase activity in transgenic mice. *Genesis* *26*, 130-132

Galli-Resta, L., Novelli, E., and Viegi, A. (2002). Dynamic microtubule-dependent interactions position homotypic neurones in regular monolayered arrays during retinal development. *Development* *129*, 3803-3814

Galli-Resta, L., Resta, G., Tan, S.S., and Reese, B.E. (1997). Mosaics of islet-1-expressing amacrine cells assembled by short-range cellular interactions. *The Journal of Neuroscience* *17*, 7831-7838

Gnanaguru, G., Bachay, G., Biswas, S., Pinzon-Duarte, G., Hunter, D.D., and Brunken, W.J. (2013). Laminins containing the beta2 and gamma3 chains regulate astrocyte migration and angiogenesis in the retina. *Development* *140*, 2050-2060. PMC3631977. 10.1242/dev.087817

Godfrey, C., Foley, A.R., Clement, E., and Muntoni, F. (2011). Dystroglycanopathies: coming into focus. *Current Opinion in Genetics & Development* *21*, 278-285. 10.1016/j.gde.2011.02.001

Halfter, W., Reckhaus, W., and Kroger, S. (1987). Nondirected axonal growth on basal lamina from avian embryonic neural retina. *The Journal of Neuroscience* *7*, 3712-3722

Halfter, W., Willem, M., and Mayer, U. (2005). Basement membrane-dependent survival of retinal ganglion cells. *Invest Ophthalmol Vis Sci* *46*, 1000-1009. 10.1167/iovs.04-1185

Huckfeldt, R.M., Schubert, T., Morgan, J.L., Godinho, L., Di Cristo, G., Huang, Z.J., and Wong, R.O.L. (2009). Transient neurites of retinal horizontal cells exhibit columnar tiling via homotypic interactions. *Nature Neuroscience* *12*, 35-43. 10.1038/nn.2236

Icha, J., Kunath, C., Rocha-Martins, M., and Norden, C. (2016). Independent modes of ganglion cell translocation ensure correct lamination of the zebrafish retina. *J Cell Biol* *215*, 259-275. PMC5084647. 10.1083/jcb.201604095

Kay, J.N., Chu, M.W., and Sanes, J.R. (2012). MEGF10 and MEGF11 mediate homotypic interactions required for mosaic spacing of retinal neurons. *Nature* *483*, 465-469. PMC3310952. 10.1038/nature10877

Kay, J.N., Roeser, T., Mumm, J.S., Godinho, L., Mrejeru, A., Wong, R.O.L., and Baier, H. (2004). Transient requirement for ganglion cells during assembly of retinal synaptic layers. *Development* *131*, 1331-1342. 10.1242/dev.01040

Lee, Y., Kameya, S., Cox, G.A., Hsu, J., Hicks, W., Maddatu, T.P., Smith, R.S., Naggert, J.K., Peachey, N.S., and Nishina, P.M. (2005). Ocular abnormalities in Large(myd) and Large(vls) mice, spontaneous models for muscle, eye, and brain diseases. *Mol Cell Neurosci* *30*, 160-172. 10.1016/j.mcn.2005.07.009

Li, S., Sukeena, J.M., Simmons, a.B., Hansen, E.J., Nuhn, R.E., Samuels, I.S., and Fuerst, P.G. (2015). DSCAM Promotes Refinement in the Mouse Retina through Cell Death and Restriction of Exploring Dendrites. *Journal of Neuroscience* *35*, 5640-5654. 10.1523/JNEUROSCI.2202-14.2015

Livesey, F.J., and Cepko, C.L. (2001). Vertebrate neural cell-fate determination: lessons from the retina. *Nature Reviews Neuroscience* *2*, 109-118. 10.1038/35053522

Marcos, S., Nieto-Lopez, F., Sandonis, A., Cardozo, M.J., Marco, F.D., Esteve, P., and Bovolenta, P. (2015). Secreted frizzled related proteins modulate pathfinding and fasciculation of

mouse retina ganglion cell axons by direct and indirect mechanisms. *The Journal Neuroscience* 35, 4729-4740. 10.1523/JNEUROSCI.3304-13.2015

Montanaro, F., Carbonetto, S., Campbell, K.P., and Lindenbaum, M. (1995). Dystroglycan expression in the wild type and mdx mouse neural retina: synaptic colocalization with dystrophin, dystrophin-related protein but not laminin. *Journal of Neuroscience Research* 42, 528-538. 10.1002/jnr.490420411

Moore, C.J., and Winder, S.J. (2010). Dystroglycan versatility in cell adhesion: a tale of multiple motifs. *Cell Communication and Signaling* 8, 3. 10.1186/1478-811X-8-3

Moore, C.J., and Winder, S.J. (2012). The inside and out of dystroglycan post-translational modification. *Neuromuscular Disorders* 22, 959-965. 10.1016/j.nmd.2012.05.016

Moore, S.A., Saito, F., Chen, J., Michele, D.E., Henry, M.D., Messing, A., Cohn, R.D., Ross-Barta, S.E., Westra, S., Williamson, R.A., *et al.* (2002). Deletion of brain dystroglycan recapitulates aspects of congenital muscular dystrophy. *Nature* 418, 422-425. 10.1038/nature00838

Morgan, J., and Wong, R. (1995). Development of Cell Types and Synaptic Connections in the Retina. In *Webvision: The Organization of the Retina and Visual System*, H. Kolb, E. Fernandez, and R. Nelson, eds. (Salt Lake City (UT)).

Myshrall, T.D., Moore, S.A., Ostendorf, A.P., Satz, J.S., Kowalczyk, T., Nguyen, H., Daza, R.A., Lau, C., Campbell, K.P., and Hevner, R.F. (2012). Dystroglycan on radial glia end feet is required for pial basement membrane integrity and columnar organization of the developing cerebral cortex. *J Neuropathol Exp Neurol* 71, 1047-1063. PMC3512206. 10.1097/NEN.0b013e318274a128

Nakagawa, N., Yagi, H., Kato, K., Takematsu, H., and Oka, S. (2015). Ectopic clustering of Cajal-Retzius and subplate cells is an initial pathological feature in Pomgnt2-knockout mice, a model of dystroglycanopathy. *Scientific Reports* 5, 11163. PMC4461912. 10.1038/srep11163

Omori, Y., Araki, F., Chaya, T., Kajimura, N., Irie, S., Terada, K., Muranishi, Y., Tsujii, T., Ueno, S., Koyasu, T., *et al.* (2012). Presynaptic dystroglycan-pikachurin complex regulates the proper synaptic connection between retinal photoreceptor and bipolar cells. *The Journal Neuroscience* 32, 6126-6137. 10.1523/JNEUROSCI.0322-12.2012

Ott, H., Bastmeyer, M., and Stuermer, C.A. (1998). Neurolin, the goldfish homolog of DM-GRASP, is involved in retinal axon pathfinding to the optic disk. *The Journal of Neuroscience* 18, 3363-3372

Pan, L., Deng, M., Xie, X., and Gan, L. (2008). ISL1 and BRN3B co-regulate the differentiation of murine retinal ganglion cells. *Development* 135, 1981-1990. 10.1242/dev.010751

Petros, T.J., Rebsam, A., and Mason, C.A. (2008). Retinal axon growth at the optic chiasm: to cross or not to cross. *Annual Review of Neuroscience* 31, 295-315.
10.1146/annurev.neuro.31.060407.125609

Pinzon-Duarte, G., Daly, G., Li, Y.N., Koch, M., and Brunken, W.J. (2010). Defective formation of the inner limiting membrane in laminin beta2- and gamma3-null mice produces retinal dysplasia. *Invest Ophthalmol Vis Sci* 51, 1773-1782. PMC2868416. 10.1167/iovs.09-4645

Randlett, O., Poggi, L., Zolessi, F.R., and Harris, W.A. (2011). The oriented emergence of axons from retinal ganglion cells is directed by laminin contact in vivo. *Neuron* 70, 266-280.
10.1016/j.neuron.2011.03.013

Reese, B.E. (2011). Development of the retina and optic pathway. *Vision research* 51, 613-632. 10.1016/j.visres.2010.07.010

Reese, B.E., Necessary, B.D., Tam, P.P., Faulkner-Jones, B., and Tan, S.S. (1999). Clonal expansion and cell dispersion in the developing mouse retina. *Eur J Neurosci* 11, 2965-2978

Riccomagno, M.M., Sun, L.O., Brady, C.M., Alexandropoulos, K., Seo, S., Kurokawa, M., and Kolodkin, A.L. (2014). Cas adaptor proteins organize the retinal ganglion cell layer downstream of integrin signaling. *Neuron* 81, 779-786. 10.1016/j.neuron.2014.01.036

Rohrer, B., LaVail, M.M., Jones, K.R., and Reichardt, L.F. (2001). Neurotrophin receptor TrkB activation is not required for the postnatal survival of retinal ganglion cells in vivo. *Exp Neurol* 172, 81-91. 10.1006/exnr.2001.7795

Sato, S., Omori, Y., Katoh, K., Kondo, M., Kanagawa, M., Miyata, K., Funabiki, K., Koyasu, T., Kajimura, N., Miyoshi, T., *et al.* (2008). Pikachurin, a dystroglycan ligand, is essential for photoreceptor ribbon synapse formation. *Nature Neuroscience* 11, 923-931.
10.1038/nn.2160

Satz, J.S., Barresi, R., Durbeej, M., Willer, T., Turner, A., Moore, S.A., and Campbell, K.P. (2008). Brain and eye malformations resembling Walker-Warburg syndrome are recapitulated in mice by dystroglycan deletion in the epiblast. *The Journal of Neuroscience* 28, 10567-10575. 10.1523/JNEUROSCI.2457-08.2008

Satz, J.S., Ostendorf, A.P., Hou, S., Turner, A., Kusano, H., Lee, J.C., Turk, R., Nguyen, H., Ross-Barta, S.E., Westra, S., *et al.* (2010). Distinct functions of glial and neuronal dystroglycan in the developing and adult mouse brain. *The Journal of Neuroscience* 30, 14560-14572.
10.1523/JNEUROSCI.3247-10.2010

Satz, J.S., Philp, A.R., Nguyen, H., Kusano, H., Lee, J., Turk, R., Riker, M.J., Hernández, J., Weiss, R.M., Anderson, M.G., *et al.* (2009). Visual impairment in the absence of dystroglycan. *The Journal of Neuroscience* 29, 13136-13146. 10.1523/JNEUROSCI.0474-09.2009

Takahashi, H., Kanasaki, H., Igarashi, T., Kameya, S., Yamaki, K., Mizota, A., Kudo, A., Miyagoe-Suzuki, Y., Takeda, S., and Takahashi, H. (2011). Reactive gliosis of astrocytes and Muller glial cells in retina of POMGnT1-deficient mice. *Mol Cell Neurosci* 47, 119-130. 10.1016/j.mcn.2011.03.006

Takeda, S., Kondo, M., Sasaki, J., Kurahashi, H., Kano, H., Arai, K., Misaki, K., Fukui, T., Kobayashi, K., Tachikawa, M., *et al.* (2003). Fukutin is required for maintenance of muscle integrity, cortical histiogenesis and normal eye development. *Hum Mol Genet* 12, 1449-1459

Taniguchi-Ikeda, M., Morioka, I., Iijima, K., and Toda, T. (2016). Mechanistic aspects of the formation of alpha-dystroglycan and therapeutic research for the treatment of alpha-dystroglycanopathy: A review. *Mol Aspects Med* 51, 115-124. 10.1016/j.mam.2016.07.003

Tao, C., and Zhang, X. (2016). Retinal Proteoglycans Act as Cellular Receptors for Basement Membrane Assembly to Control Astrocyte Migration and Angiogenesis. *Cell Rep* 17, 1832-1844. PMC5129871. 10.1016/j.celrep.2016.10.035

Taylor, L., Arner, K., Engelsberg, K., and Ghosh, F. (2015). Scaffolding the retina: the interstitial extracellular matrix during rat retinal development. *Int J Dev Neurosci* 42, 46-58. 10.1016/j.ijdevneu.2015.03.002

Thompson, H., Camand, O., Barker, D., and Erskine, L. (2006). Slit proteins regulate distinct aspects of retinal ganglion cell axon guidance within dorsal and ventral retina. *The Journal of Neuroscience* 26, 8082-8091. 10.1523/JNEUROSCI.1342-06.2006

Tronche, F., Kellendonk, C., Kretz, O., Gass, P., Anlag, K., Orban, P.C., Bock, R., Klein, R., and Schutz, G. (1999). Disruption of the glucocorticoid receptor gene in the nervous system results in reduced anxiety. *Nat Genet* 23, 99-103. 10.1038/12703

Varshney, S., Hunter, D.D., and Brunken, W.J. (2015). Extracellular Matrix Components Regulate Cellular Polarity and Tissue Structure in the Developing and Mature Retina. *J Ophthalmic Vis Res* 10, 329-339. PMC4687269. 10.4103/2008-322X.170354

Wang, S.W., Kim, B.S., Ding, K., Wang, H., Sun, D., Johnson, R.L., Klein, W.H., and Gan, L. (2001). Requirement for math5 in the development of retinal ganglion cells. *Genes Dev* 15, 24-29. PMC312600

Wassle, H., and Riemann, H.J. (1978). The mosaic of nerve cells in the mammalian retina. *Proc R Soc Lond B Biol Sci* 200, 441-461

Wright, K.M., Lyon, K.A., Leung, H., Leahy, D.J., Ma, L., and Ginty, D.D. (2012). Dystroglycan organizes axon guidance cue localization and axonal pathfinding. *Neuron* 76, 931-944. 10.1016/j.neuron.2012.10.009

Xiao, T., Staub, W., Robles, E., Gosse, N.J., Cole, G.J., and Baier, H. (2011). Assembly of lamina-specific neuronal connections by slit bound to type IV collagen. *Cell* 146, 164-176. PMC3136219. 10.1016/j.cell.2011.06.016

Xu, H.P., Burbridge, T.J., Ye, M., Chen, M., Ge, X., Zhou, Z.J., and Crair, M.C. (2016). Retinal Wave Patterns Are Governed by Mutual Excitation among Starburst Amacrine Cells and Drive the Refinement and Maintenance of Visual Circuits. *The Journal of Neuroscience* 36, 3871-3886. PMC4812142. 10.1523/JNEUROSCI.3549-15.2016

Yang, L., Cai, C.L., Lin, L., Qyang, Y., Chung, C., Monteiro, R.M., Mummery, C.L., Fishman, G.I., Cogen, A., and Evans, S. (2006). *Isl1*Cre reveals a common Bmp pathway in heart and limb development. *Development* 133, 1575-1585. 10.1242/dev.02322

Young, R.W. (1984). Cell death during differentiation of the retina in the mouse. *J Comp Neurol* 229, 362-373. 10.1002/cne.902290307

Yurchenco, P.D. (2011). Basement membranes: cell scaffoldings and signaling platforms. *Cold Spring Harb Perspect Biol* 3. PMC3039528. 10.1101/cshperspect.a004911

Figure 1

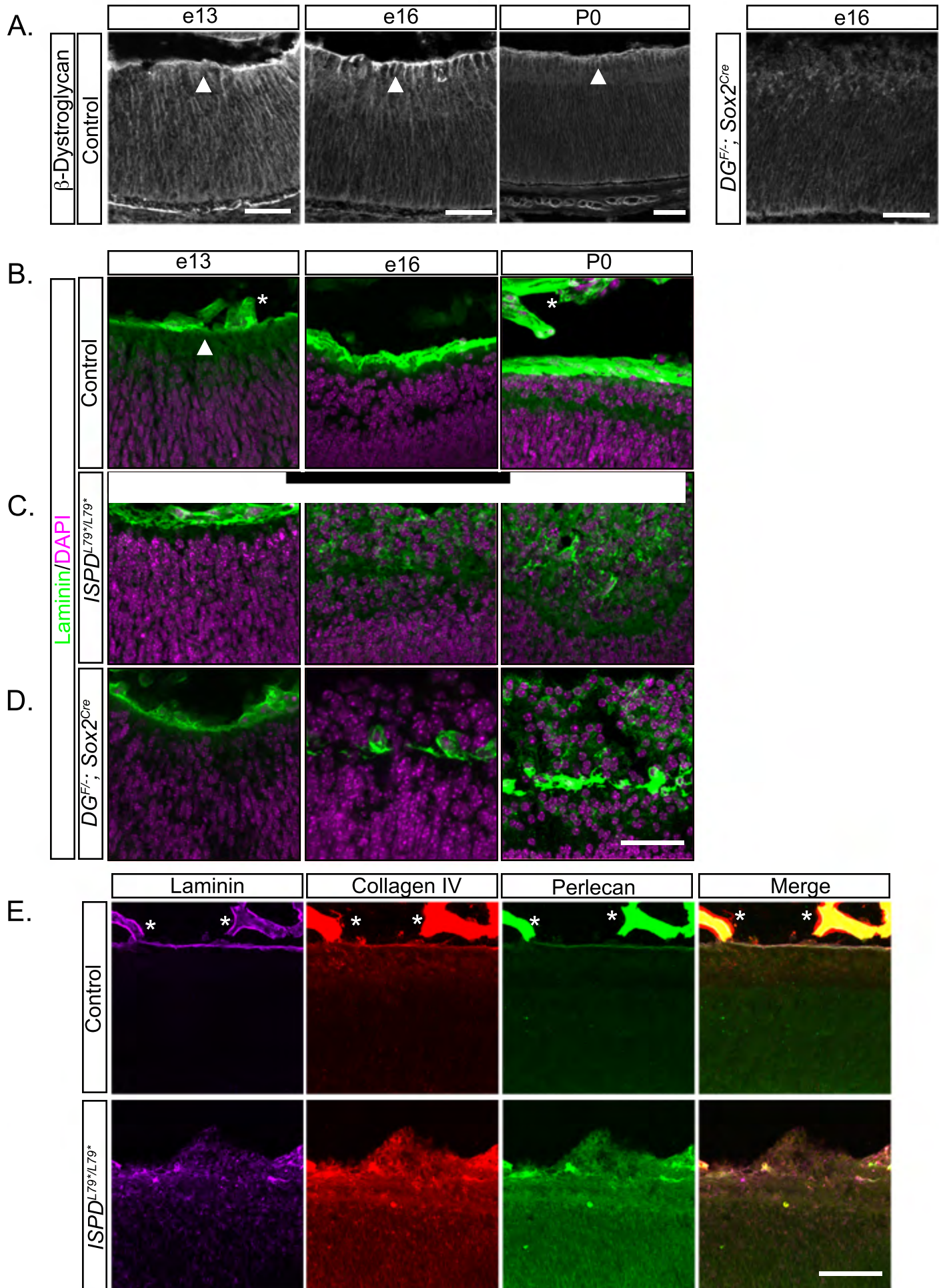


Figure 2

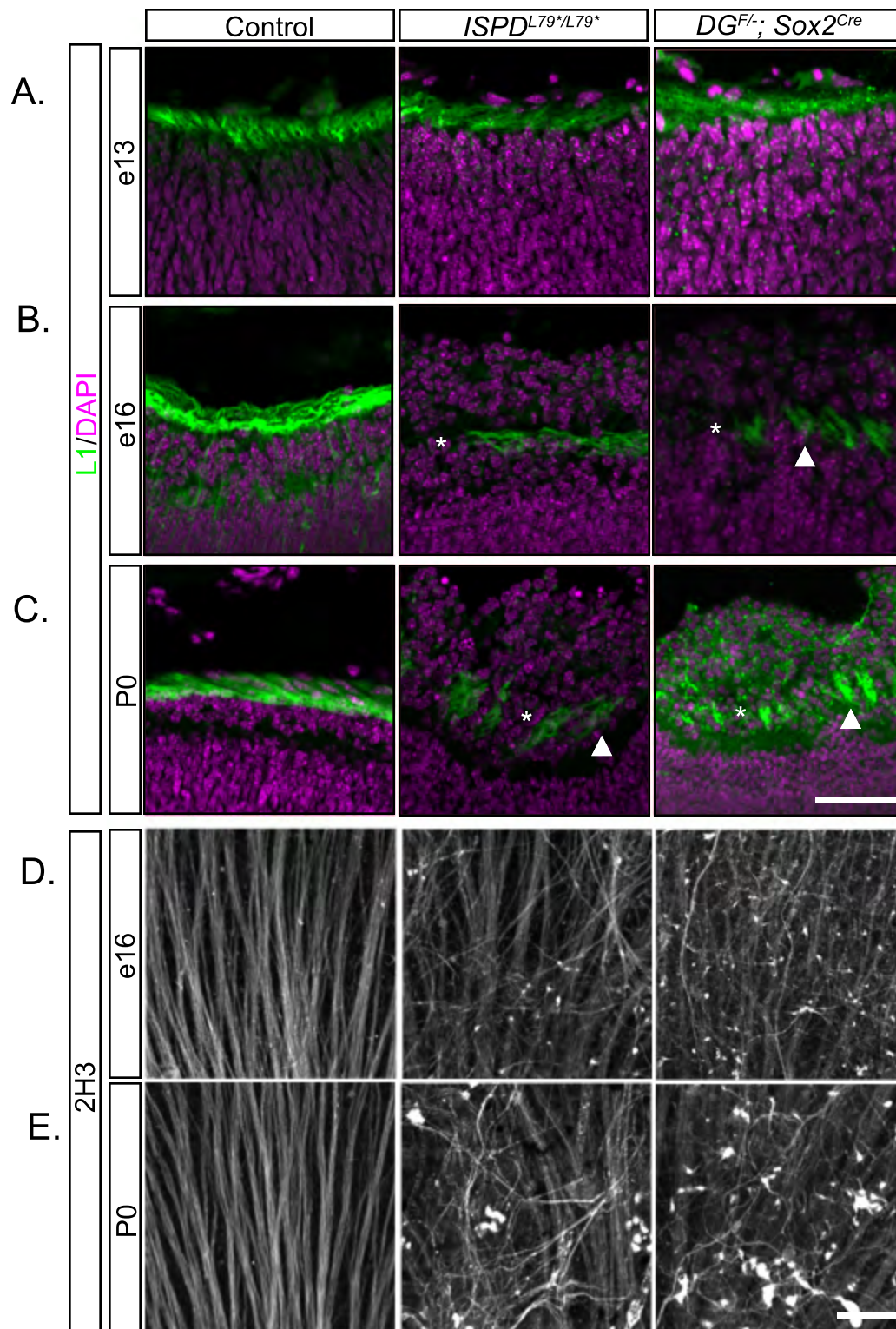


Figure 3

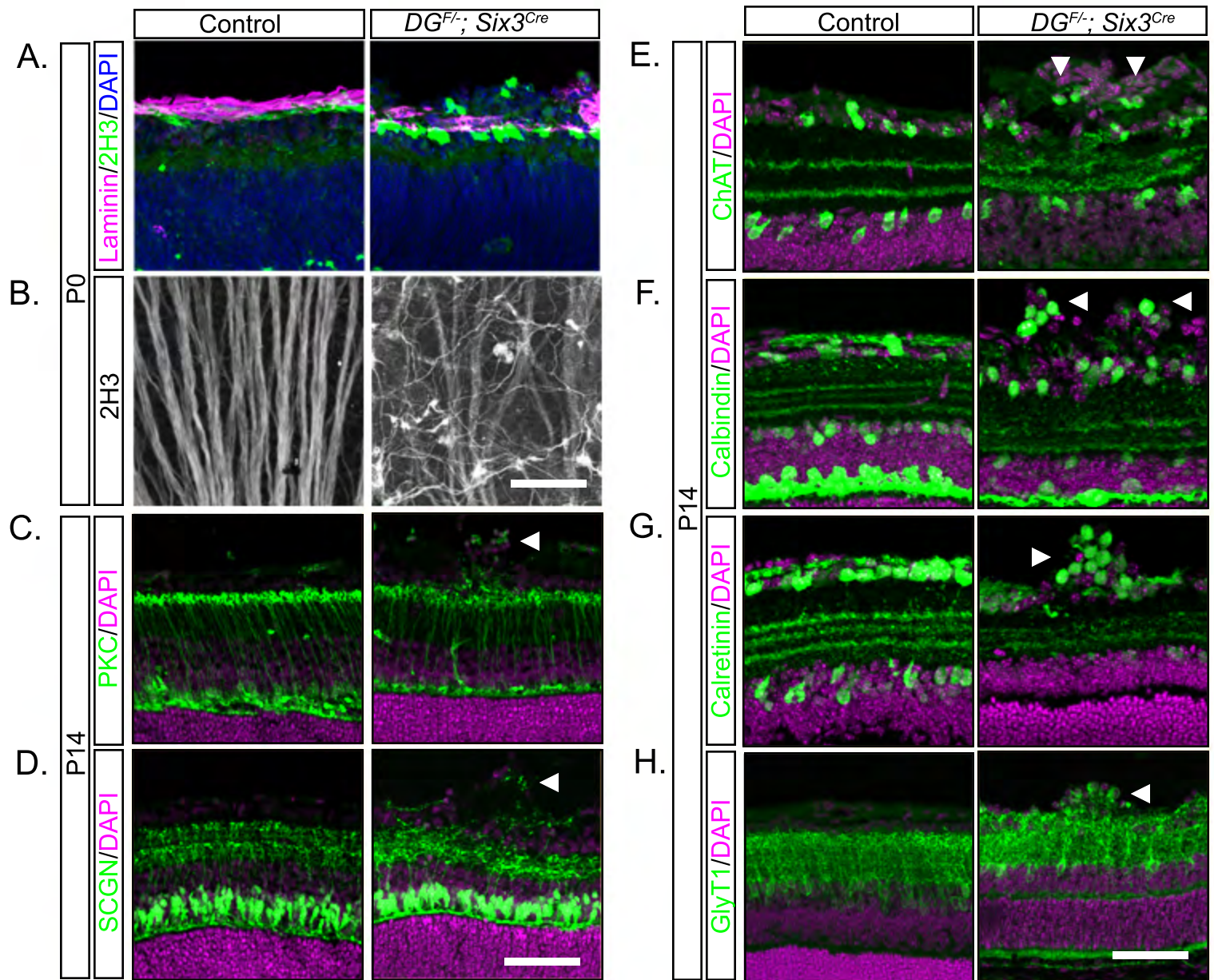


Figure 4

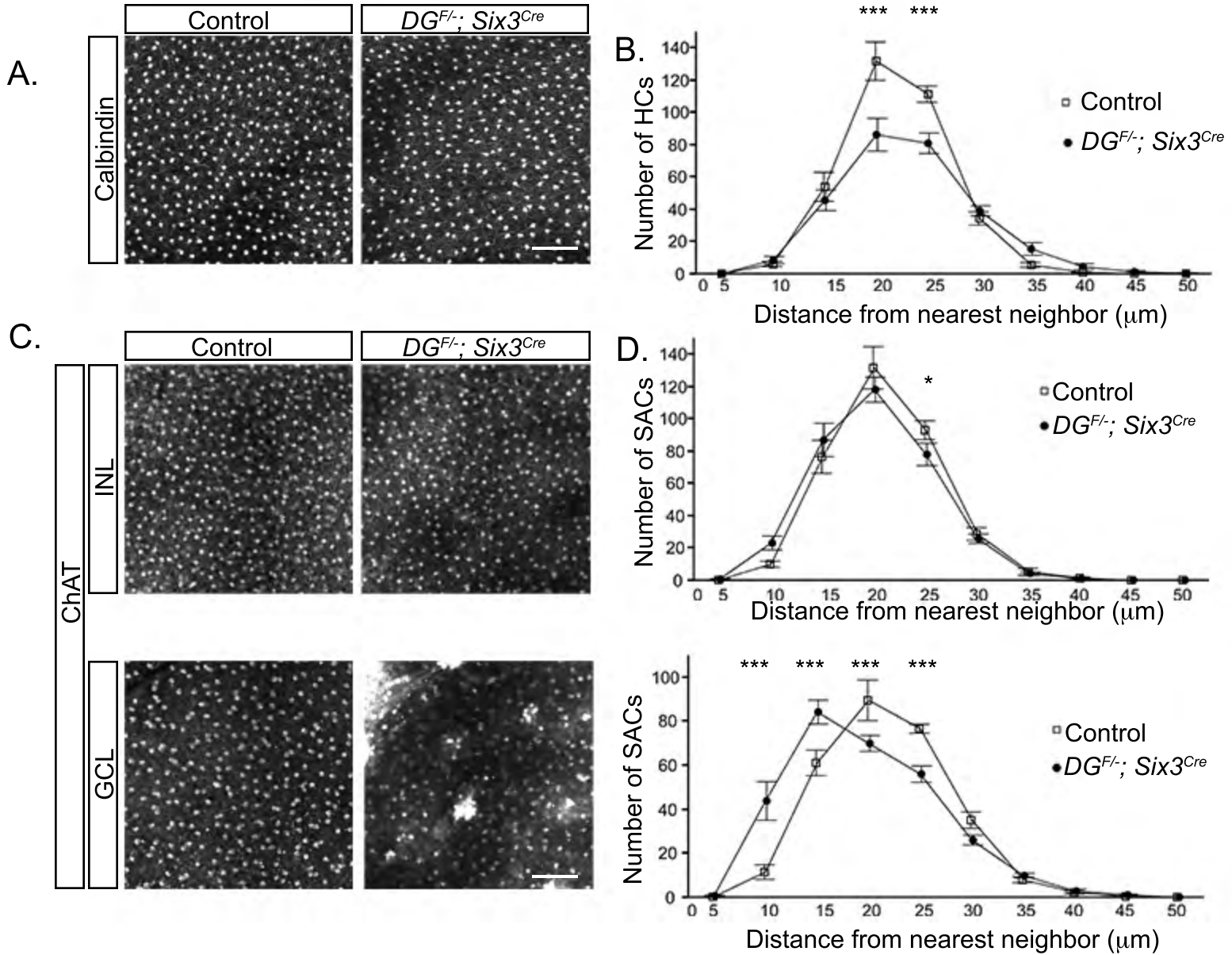


Figure 5

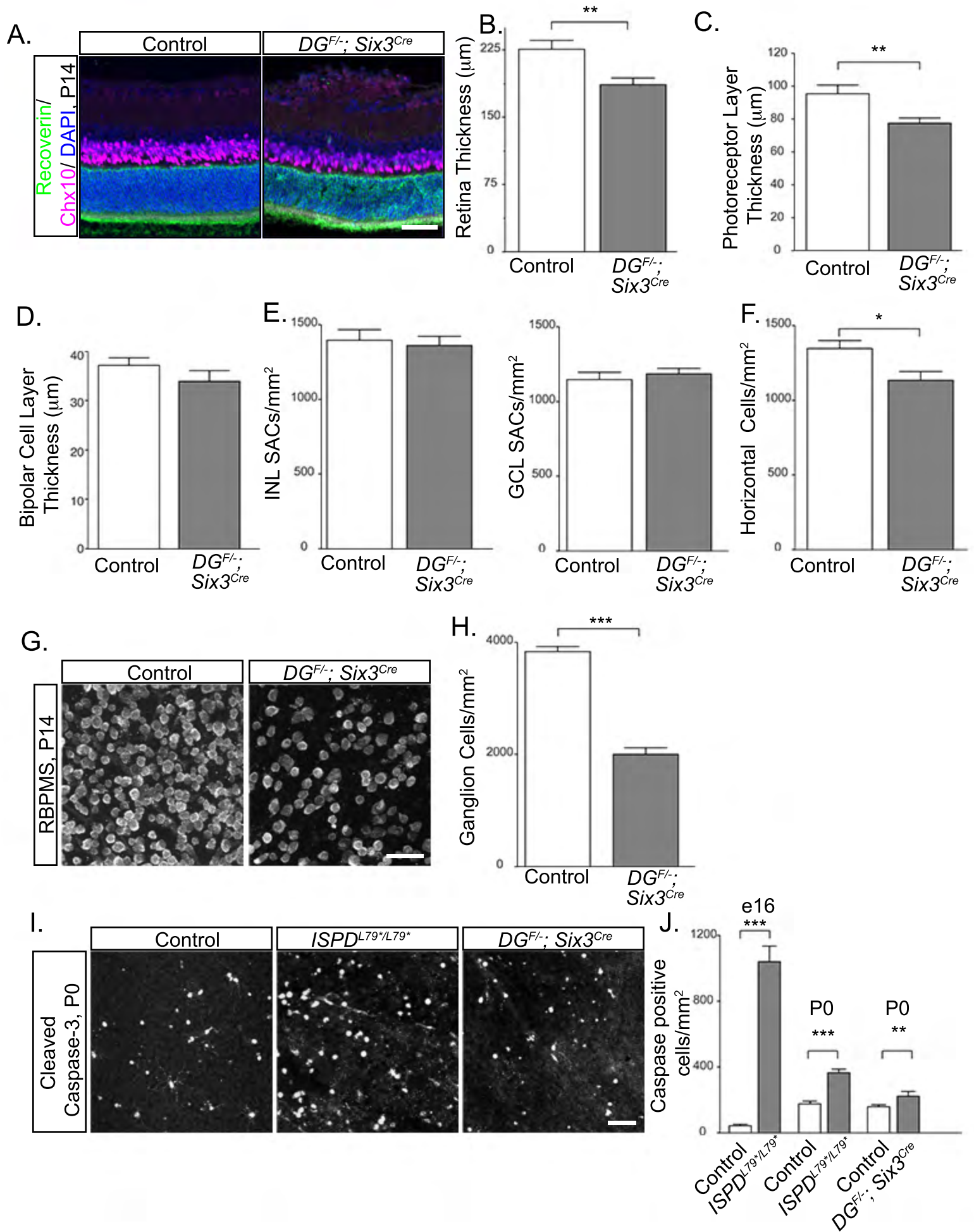


Figure 6

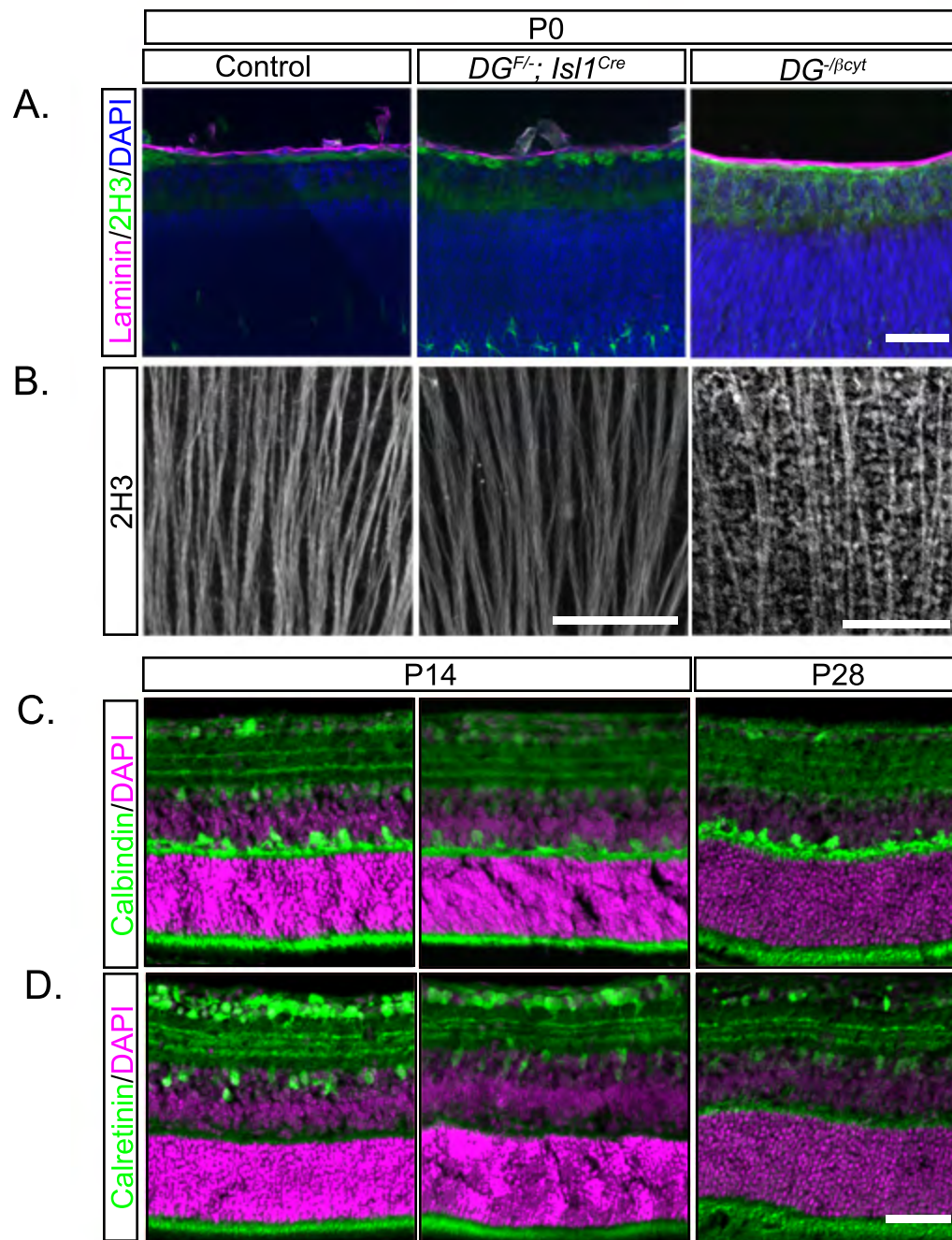


Figure 7

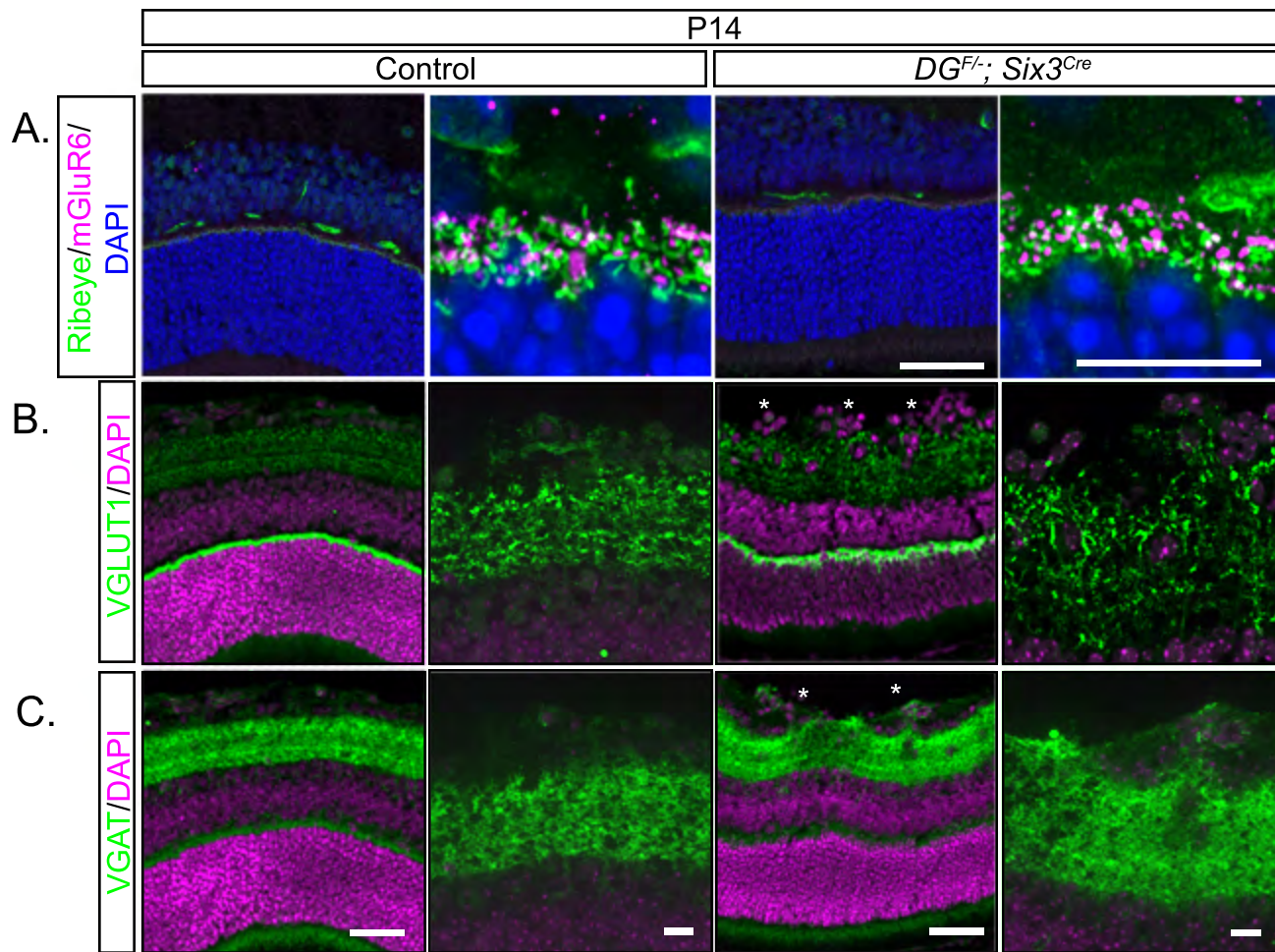
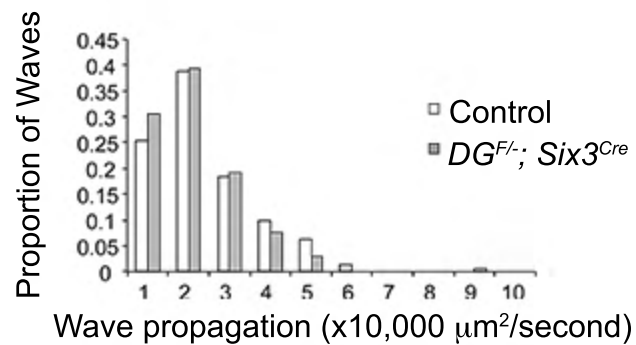
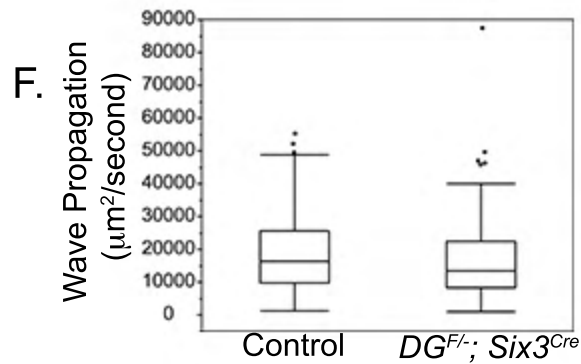
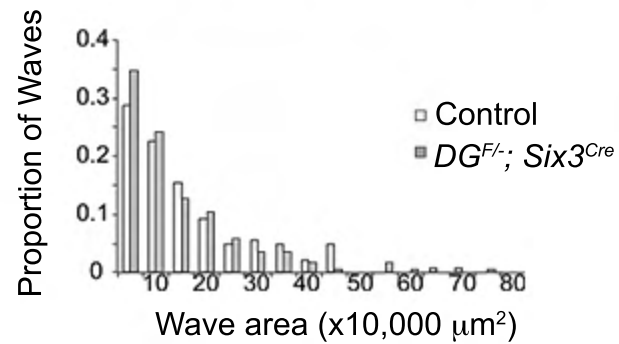
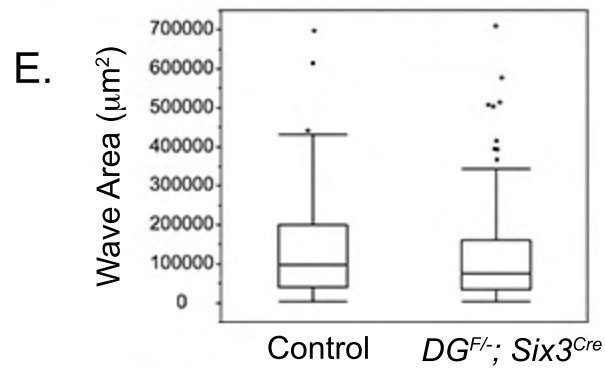
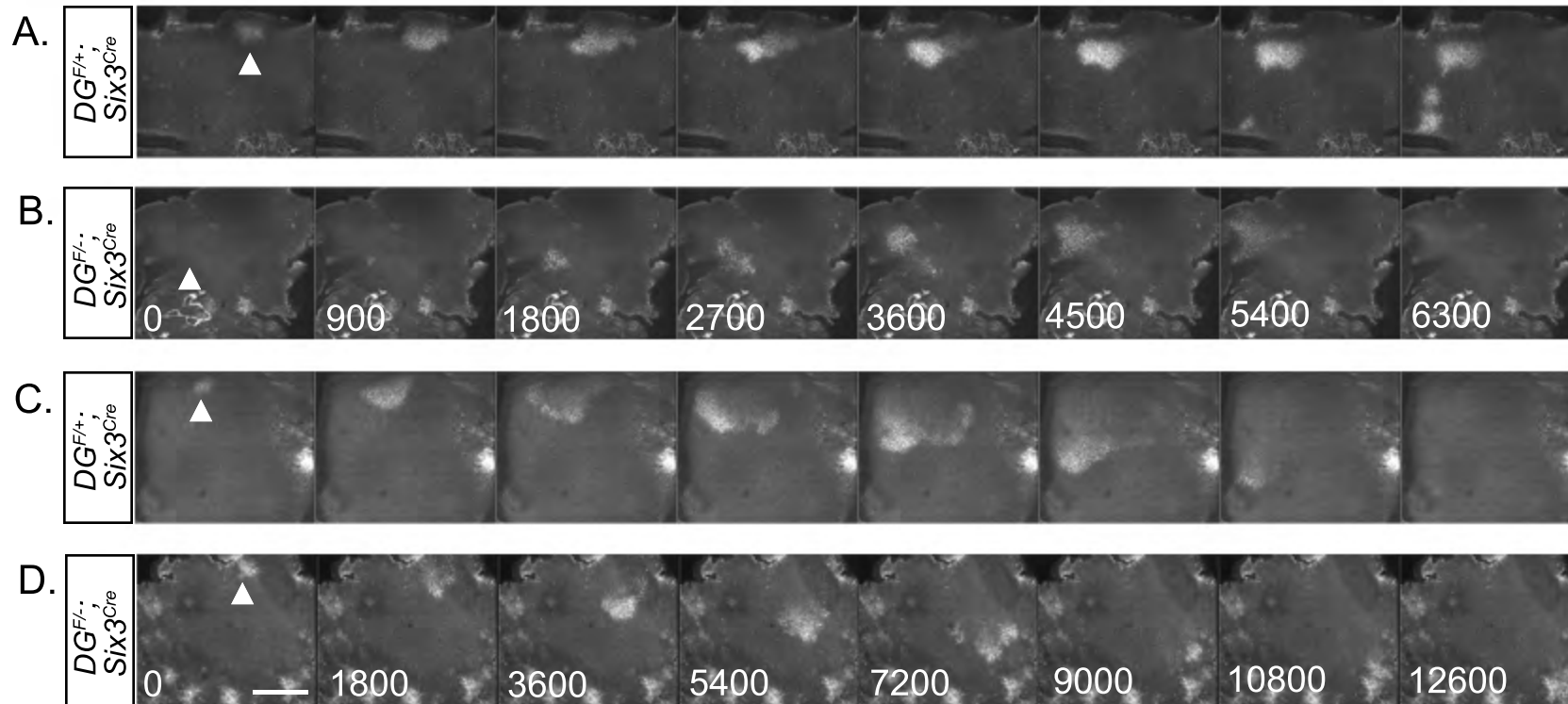


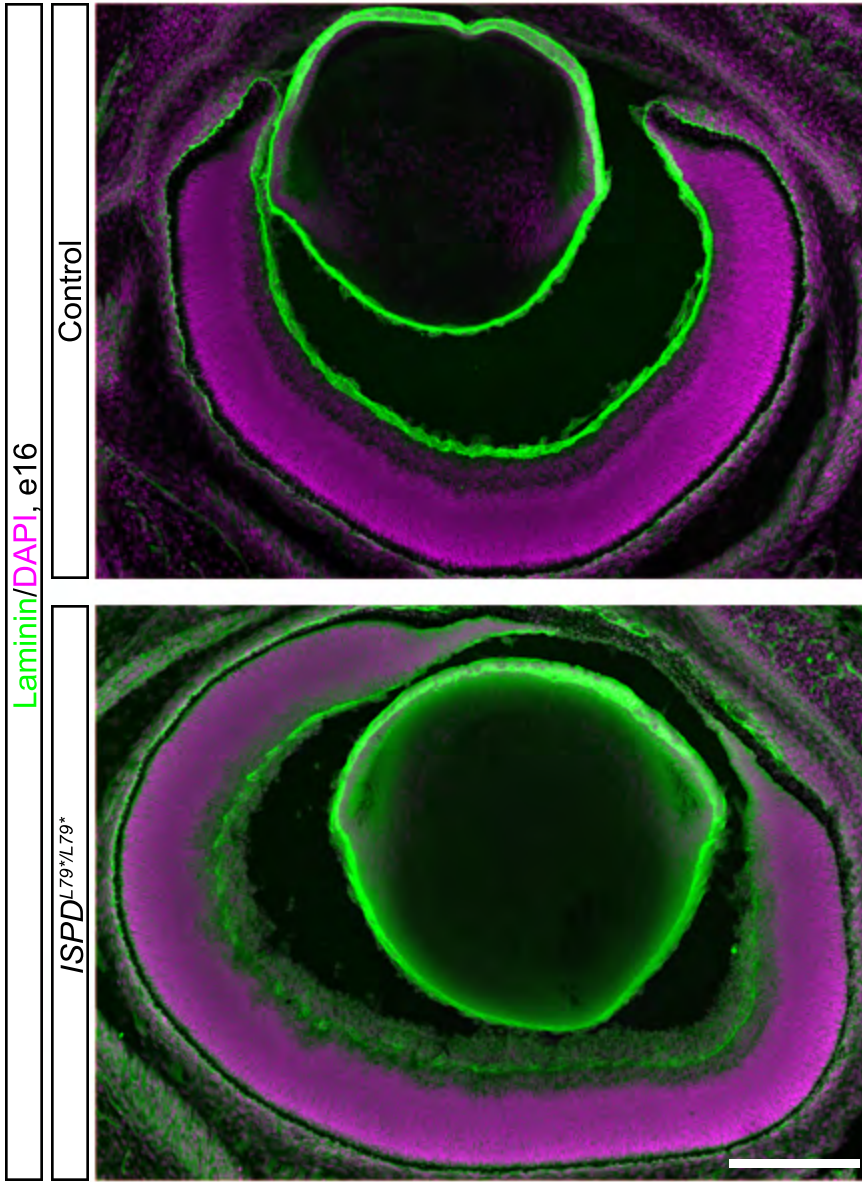
Figure 8



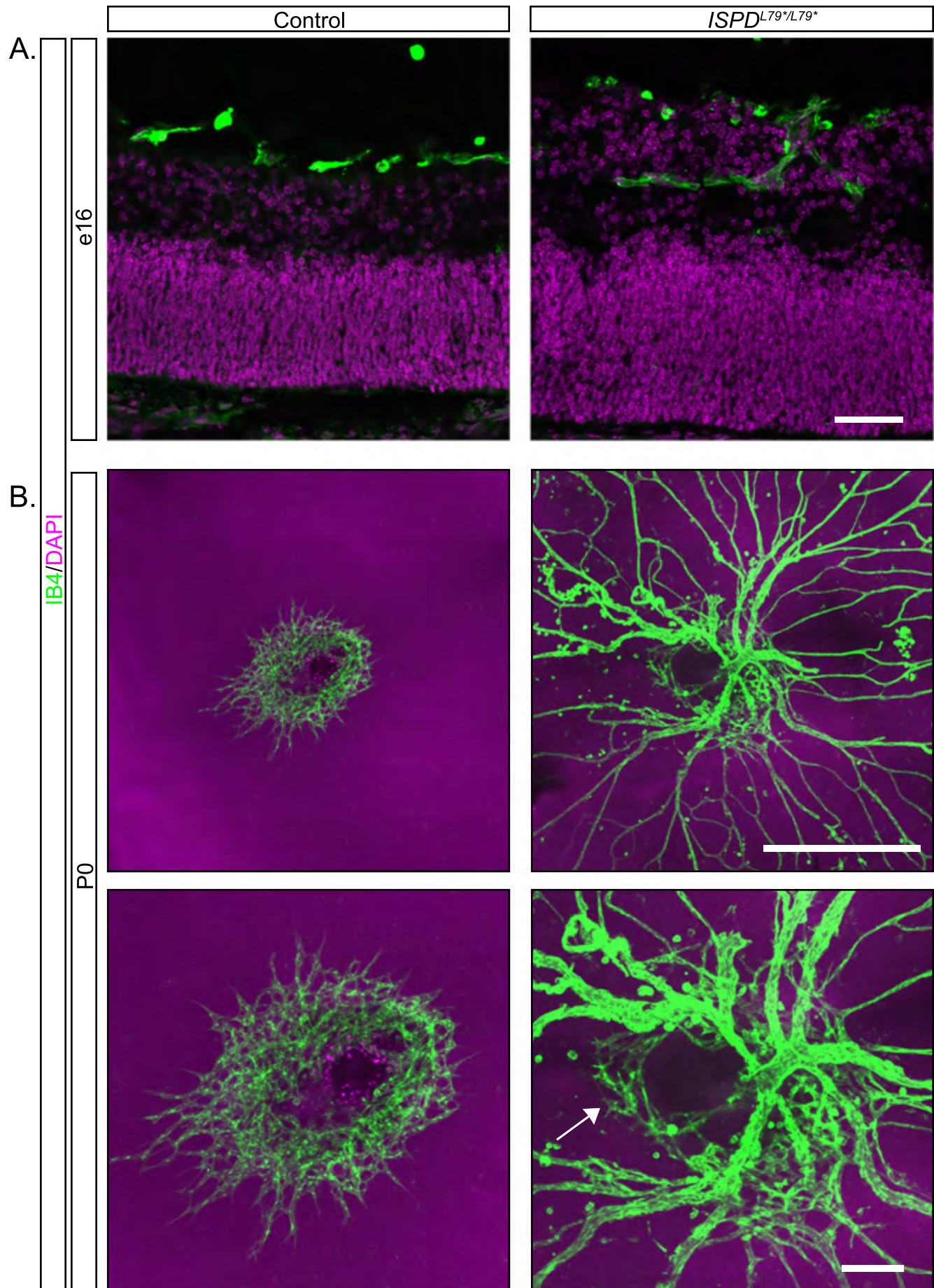
Supplemental Table 1

Target	Host species	Dilution	Company/origin	Catalog #	RRID
Beta DG	rabbit	1:100	Santa Cruz Biotech	sc-28535	AB_782259
Laminin	rabbit	1:1000	Sigma	L9393	AB_477163
Collagen IV	goat	1:250	Southern Biotech	1340-01	AB_2082646
Perlecan	rat	1:500	Millipore	MAB1948P	AB_10615958
L1	rat	1:500	Millipore	MAB5272	AB_2133200
2H3	mouse	1:1000	DSHB	2h3	AB_531793
ChAT	goat	1:500	Millipore	AB144P-200UL	AB_11214092
Calbindin	rabbit	1:10,000	Swant	CB 38	AB_10000340
Calretinin	rabbit	1:10,000	Swant	CG 1	AB_2619710
GlyT1	rabbit	1:800	gift from Dr. David Pow		
PKC	mouse	1:500	Sigma	P5704	AB_477375
Secretagogen	rabbit	1:4000	Biovendor	rd181120100	AB_2034060
Recoverin	rabbit	1:200	Millipore	AB5585	AB_2253622
Chx10	goat	1:500	Santa Cruz Biotech	sc-21690	AB_2216006
RBPMS	guinea pig	1:500	PhosphoSolutions	1832-RBPMS	AB_2492226
Cleaved Caspase-3	rabbit	1:500	Cell Signaling	9661S	AB_2341188
Ribeye/Ctbp2	mouse	1:1000	BD Biosciences	612044	AB_399431
MGlur6	sheep	1:100	gift from Dr. Catherine Morgans		
VGLUT1	guinea pig	1:500	Millipore	AB5905	AB_2301751
VGAT	rabbit	1:500	Synaptic Systems	131-003	AB_887869

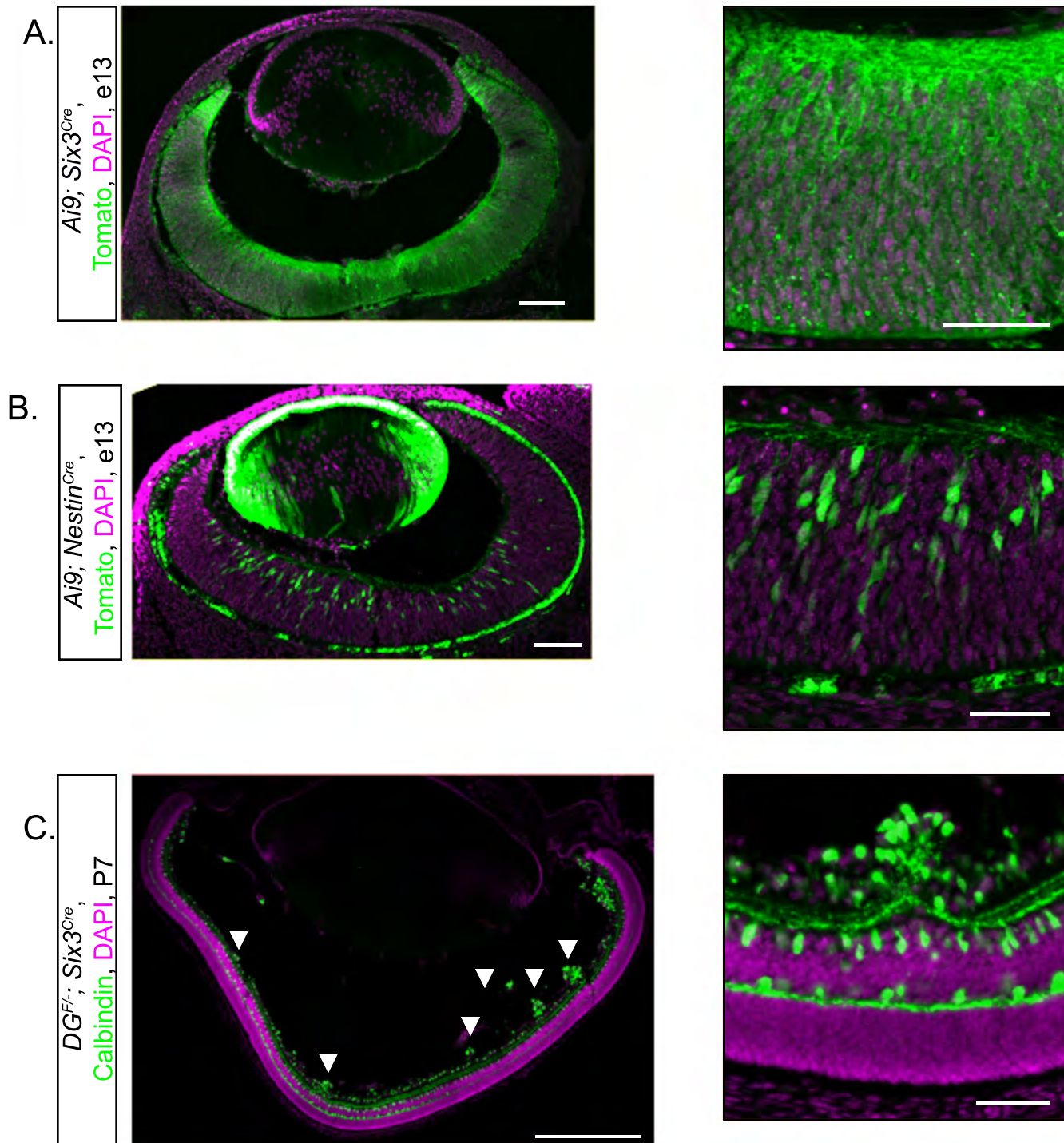
Supplemental Figure 1



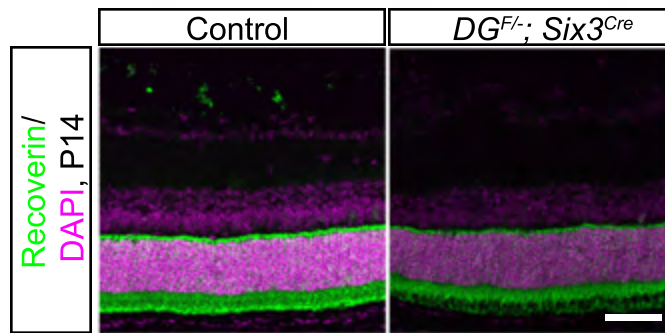
Supplemental Figure 2



Supplemental Figure 3



Supplemental Figure 4



Supplemental Figure 5

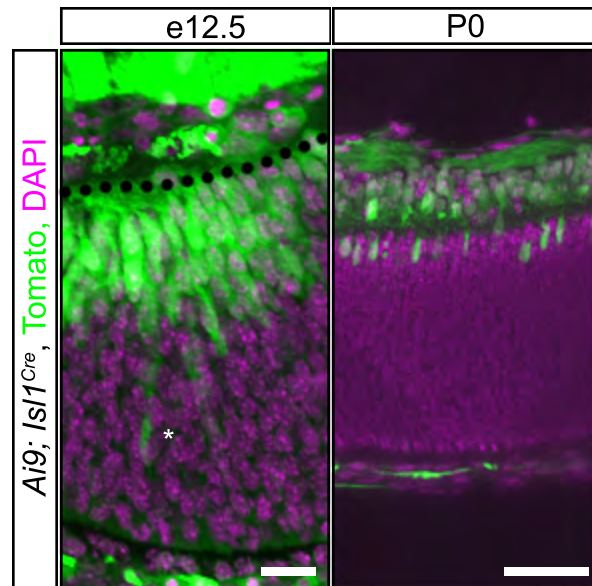


Figure Legends

Figure 1: The inner limiting membrane undergoes progressive degeneration in the absence of functional dystroglycan. (A) Dystroglycan (α -DG) is expressed throughout the developing retina, with an enrichment at the inner limiting membrane (ILM). Dystroglycan expression is lost in $DG^{F/-}; Sox2^{Cre}$ mice (right). (B-D) The initial assembly of the ILM occurs normally in the absence of functional dystroglycan in (C) $ISPD^{L79*/L79*}$ and (D) $DG^{F/-}; Sox2^{Cre}$ retinas. The ILM in $ISPD^{L79*/L79*}$ and $DG^{F/-}; Sox2^{Cre}$ retinas undergoes progressive degeneration at e16 (middle) and P0 (right), and retinal neurons migrate into the vitreous. (E) Localization of multiple extracellular matrix proteins, including laminin (purple), collagen IV (red), and perlecan (green), is disrupted in the ILM in the absence of functional dystroglycan in $ISPD^{L79*/L79*}$ retinas at P0. Arrowheads indicate ILM, asterisks indicate blood vessels. Scale bar, 50 μ m.

Figure 2: Dystroglycan is required for intraretinal axon guidance (A) L1 positive axons in the optic fiber layer (OFL) initially appear normal in $ISPD^{L79*/L79*}$ (middle), and $DG^{F/-}; Sox2^{Cre}$ retinas (right) at e13. (B, C) As the ILM degenerates in $ISPD^{L79*/L79*}$ and $DG^{F/-}; Sox2^{Cre}$ retinas at e16 (B) and P0 (C), axons hyperfasciculate (arrowhead) and exhibit gaps (asterisk) within the OFL. (D, E). Flat mount preparations from $ISPD^{L79*/L79*}$ and $DG^{F/-}; Sox2^{Cre}$ retinas at e16 (D) and P0 (E) show progressive disruption of axon tracts (Neurofilament, 2H3). Scale bar, 50 μ m.

Figure 3: Disrupted circuit formation in the inner retina of postnatal dystroglycan mutants. (A, B) $DG^{F/-}; Six3^{Cre}$ (right) mice exhibit inner limiting membrane degeneration (top, purple, laminin) and abnormal axonal fasciculation and guidance (top, green, bottom, 2H3). (C-D) The cell bodies of bipolar cells (PKC, C, SCGN, D) exhibit normal lamination patterns, while their axons extend into ectopic cellular clusters in the ganglion cell layer. (E-H) Abnormal cellular lamination and disruptions in dendritic stratification of multiple amacrine and retinal ganglion cell types is observed in $DG^{F/-}; Six3^{Cre}$ retinas. (E) ChAT labels starburst amacrine cells, (F) calbindin and (G) calretinin label amacrine and ganglion cells, and (H) GlyT1 labels glycinergic amacrine cells. Arrowheads indicate axons or cell bodies in ectopic clusters. Scale bar, 50 μ m.

Figure 4: Dystroglycan is required for mosaic cell spacing in the ganglion cell layer. (A, B). Horizontal cells (2H3) in flat mount P14 adult retinas have reduced cellular density, but normal mosaic cell spacing curves (Nearest neighbor analysis, Two-Way ANOVA, n=20 samples from 5 control retinas, 18 samples from 5 mutant retinas). (C, D) Mosaic cell spacing of starburst amacrine cells (ChAT) in the inner nuclear layer is normal (Nearest neighbor analysis, Two-Way ANOVA, n=10 samples from 3 control retinas, 10 samples from 3 mutant retinas), while the ectopic clustering of starburst amacrine cells in the ganglion cell layer results in a significant disruption of mosaic spacing (Nearest

neighbor analysis, Two-Way ANOVA, n=10 samples from 3 control retinas, 10 samples from 3 mutant retinas). Scale bar 100 μ m.

Figure 5: Retinal thinning in *dystroglycan* mutants. (A-D) P14 *DG^{F/-}; Six3^{cre}* retinas show decreased retinal thickness (DAPI, $p < 0.01$, n=7 control, 7 mutant), a decreased thickness of the photoreceptor layer (C, Recoverin, green, $p < 0.01$, n=7 control, 7 mutant) and no change in thickness of the bipolar cell layer (D, Chx10, purple, $p > 0.05$, n=7 control, 7 mutant). Starburst amacrine cell density is normal in both the GCL and INL (E, n=10 samples from 3 control retinas, 10 samples from 3 mutant retinas), while horizontal cells show a slight reduction in cell density (F) in P14 *DG^{F/-}; Six3^{cre}* retinas ($p < 0.05$, n=20 samples from 5 control retinas, 18 samples from 5 mutant retinas). (G,H) Ganglion cell density (RBPMS) is reduced by approximately 50% in P14 *DG^{F/-}; Six3^{cre}* retinas ($p < 0.0001$, n=12 samples from 3 control retinas, 12 samples from 3 mutant retinas). (I-J) Immunohistochemistry for cleaved caspase-3 in a flat mount preparation of P0 *DG^{F/-}; Six3^{cre}* retinas shows an increase in apoptotic cells. (t test, $p < 0.05$, n=18 samples from 6 control retinas, 17 samples from 6 mutant retinas). (J) Quantification of cleaved caspase-3 positive cells shows an increase in apoptotic cells at e16 (t test, $p < 0.0001$, n=18 samples from 6 control retinas, 18 samples from 8 mutant retinas) and P0 (I,J t test, $p < 0.0001$, n=18 samples from 6 control retinas, 15 samples from 5 mutant retinas) between control (left) and *ISPD^{L79*/L79*}* (middle) retinas. Scale bar 50 μ m.

Figure 6: Dystroglycan functions non-cell autonomously and does not require its intracellular signaling domain for retinal development. (A) The ILM (laminin, purple) and axons in the OFL (2H3, green) appear similar to control in *DG^{F/-}; Isl1^{cre}* (middle panel) retinas and mice lacking the intracellular domain of dystroglycan (*DG^{-/βcyt}*) (right panel) retinas at P0. (B) Flat mount preparations show normal axon fasciculation (2H3) in *DG^{F/-}; Isl1^{cre}* (middle panel) retinas and *DG^{-/βcyt}* (right panel) retinas. (C-D) *DG^{F/-}; Isl1^{cre}* (middle panel) retinas (P14) and *DG^{-/βcyt}* (right panel) retinas (P28) have normal cellular lamination and dendritic stratification. Scale bar, 50 μ m.

Figure 7: Dystroglycan is dispensable for synapse formation in the retina. (A) Markers for outer retinal ribbon synapses (Ribeye, presynaptic and mGluR6, postsynaptic) appear structurally normal in the absence of dystroglycan. The density of (B) excitatory (VGLUT1) and (C) inhibitory (VGAT) presynaptic markers appear similar to control in the inner retinas of *DG^{F/-}; Six3^{cre}* mutants. Synapses are also present within ectopic clusters (asterisks). Scale bar, 50 μ m wide view, scale bar, 10 μ m enlarged view.

Figure 8: Dystroglycan is dispensable for the generation and propagation of retinal waves. (A-D) At P1, waves propagate normally across the retina in *DG^{F/+}; Six3^{cre}; R26-LSL-GCaMP6f* (A, C) and *DG^{F/-}; Six3^{cre}; R26-LSL-GCaMP6f* mice (B, D). Both small (A, B) and large (C, D) retinal waves are present at a similar frequency in *DG^{F/+}; Six3^{cre}; R26-LSL-GCaMP6f* and *DG^{F/-}; Six3^{cre}; R26-*

LSL-GCaMP6f retinas. (E) Distributions of wave areas show no difference between controls and mutants (Wilcoxon rank sum test, $p > 0.05$). (F) Wave propagation rate is significantly slower in mutant retinas (Wilcoxon rank sum test, $p < 0.05$). Wave parameters were calculated from 142 control waves obtained from 6 retinas from 3 control mice and 173 mutant waves obtained from 8 retinas from 5 mutant mice. Arrowheads indicate the initiation site of a retinal wave. Scale bar 500 μm . Time displayed in milliseconds.

Supplemental Figure Legends

Supplemental Figure 1: Cellular migration defects encompass the entire retina in *ISPD^{L79*/L79*}* mutants. The ILM in *ISPD^{L79*/L79*}* retinas undergoes degeneration (bottom panel) that is present across the entire span of the retina at e16. Laminin, green, DAPI, purple. Scale bar, 200 μm .

Supplemental Figure 2: Dystroglycan is required for normal vasculature development. (A) IB4 labeled hyaloid vasculature is present in the vitreous adjacent to the GCL in control retinas (left) but is embedded within ectopic cell clusters *ISPD^{L79*/L79*}* (right) retinas at e16. (B) Flat mount retinas at P0 show an ingrowth of the primary vascular plexus in controls (left top and bottom). In *ISPD^{L79*/L79*}* retinas (right top and bottom), the ingrowth of the primary plexus into the retina is delayed (arrow) and there is a persistence of hyaloid vasculature. Scale bar 50 μm A, 500 μm B top, 100 μm B bottom.

Supplemental Figure 3: Deletion of *dystroglycan* throughout the developing retina results in migration defects. (A) Recombination pattern of *Rosa26-lox-stop-lox-TdTomato; Ai9* reporter (green) by *Six3^{cre}* shows expression throughout the retina and in axons at e13. (B). Recombination pattern of *Rosa26-lox-stop-lox-TdTomato; Ai9* (green) by *Nestin^{cre}* shows expression in a sparse population of differentiated retinal neurons at e13. (C). Focal migration defects (arrowheads) in P7 *DG^{F/-}; Six3^{cre}* retinas are present across the entire span of the retina. Scale bar 100 μm A, B, left, 500 μm C, left, 50 μm A, B, C, right.

Supplemental Figure 4: Lamination of outer retina is normal in *dystroglycan* mutants. Photoreceptors (recoverin, green) have normal lamination in P14 *DG^{F/-}; Six3^{cre}* retinas (right). Scale bar 50 μm .

Supplemental Figure 5: Recombination pattern of *Isl1^{cre}* in the retina. Recombination pattern of *Rosa26-lox-stop-lox-TdTomato; Ai9* reporter (green) by *Isl1^{cre}* by shows expression in a large proportion of differentiated ganglion cells at e12.5 (left) and P0 (right). Dashed line indicates ILM. Asterisk notes a differentiated ganglion cell body that is still migrating toward the ILM. Scale bar 20 μm left panel, scale bar 50 μm right panel.